AD 606666
ڔ

69

BERYLLIUM RESEARCH AND DEVELOPMENT PROGRAM

A STUDY OF THE BRITTLE BEHAVIOR OF BERYLLIUM BY MEANS OF TRANSMISSION ELECTRON MICROSCOPY

JULY 1964

AIR FORCE MATERIALS LABORATORY
RESEARCH AND TECHNOLOGY DIVISION
AIR FORCE SYSTEMS COMMAND
WRIGHT-PATTERSON AIR FORCE BASE, OHIO

DDC

OCT 12 1964

DDC IRA C

NOTICES

When Government drawings, specifications, or other data are used for any purpose other than in connection with a definitely related Government procurement operation, the United States Government thereby incurs no responsibility nor any obligation whatsoever; and the fact that the Government may have formulated, furnished, or in any way supplied the said drawings, specifications, or other data, is not to be regarded by implication or otherwise as in any manner licensing the holder or any other person or corporation, or conveying any rights or permission to manufacture, use, or sell any patented invention that may in any way be related thereto.

Qualified requesters may obtain copies of this report from the Defense Documentation Center (DDC), (formerly ASTIA), Cameron Station, Bldg. 5, 5010 Duke Street, Alexandria, Virginia, 22314.

This report has been released to the Office of Technical Services, U.S. Department of Commerce, Washington 25, D. C., in stock quantities for sale to the general public.

Copies of this report should not be returned to the Research and Technology Division, Wright-Patterson Air Force Base, Ohio, unless return is required by security considerations, contractual obligations, or notice on a specific document.

700 - August 1964 - 448 - 4-83

FOREWORD

This report was prepared under USAF Contract No. AF 33(616)-7065 with Nuclear Metals, Inc., West Concord, Massachusetts, as the prime contractor. The contract was initiated under Project No. 7351, "Metallic Materials," Task No. 735104, "Beryllium and Beryllium Alloys." The work was administered under the direction of the Metals and Ceramics Division, Air Force Materials Laboratory, Research and Technology Division, with Mr. K. L. Kojola and Capt. P. S. Duletsky acting as project engineers.

The portion of the work covered by this volume was performed under Subcontract No. 4, "A Study of the Brittle Behavior of Beryllium by Means of Transmission Electron Microscopy," by The Franklin Institute Laboratories, Philadelphia, Pennsylvania. The authors of this volume are Mr. F. Wilhelm and Dr. H. G. F. Wilsdorf of The Franklin Institute Laboratories.

This report covers the period of work from 1 July 1960 to 31 March 1963.

The Air Force gratefully acknowledges the assistance provided by Dr. A. R. Kaufmann of Nuclear Metals in editing this report.

ABSTRACT

Glide dislocations in beryllium c. ·cimens were studied by direct observatio.. with an electron microscope. The procedures are described by which specimens were heat treated and deformed as well as the technique used to obtain electron-transparent specimens from bulk beryllium.

Investigations made on polycrystalline Pechiney flake beryllium, on commercial purity single crystal plates, and on high purity single crystal tensile specimens are described.

Glide dislocations in beryllium are strongly hindered in their movements and are often pinned by lattice imperfections and larger precipitate particles, especially in beryllium of commercial purity. Dislocation tangles have been observed in deformed Pechiney flake beryllium and in crystals of commercial purity; the presence of round as well as elongated prismatic dislocation loops is in evidence. Dislocations of different slip systems may react to form incipient networks. In specimens where dislocation pinning is less pronounced, dislocations have a tendency to align themselves along crystallographic directions. In high purity tensile specimens, dislocation bundles of high density are found to lie in the basal plane in a $<1\bar{1}00>$ direction perpendicular to the principal glide direction. Many of these dislocations are dipoles. It is found that most dislocation reactions are confined to relatively thin glide packets parallel to the basal plane. Rarely have dislocation motions been observed under the stress created by a high-intensity electron beam in the microscope. A high Peierls-Nabarro force as well as high stacking fault energy in beryllium is concluded. An inference is drawn with regard to the brittleness problem of beryllium.

This technical documentary report has been reviewed and is approved.
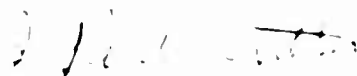
I. PERLMUTTER
Chief, Physical Metallurgy Branch
Metals and Ceramics Division
Air Force Materials Laboratory

TABLE OF CONTENTS

LIST OF ILLUSTRATIONS

I. INTRODUCTION

The purpose of this project was to investigate the behavior of dislocations in beryllium and to contribute to the understanding of the brittleness problem. The dislocation patterns in beryllium have been examined by means of transmission electron microscopy, which method require that specimens to be investigated be thinned down by appropriate techniques so that they became transparent to the electron beam in the microscope. A special technique, based on diffraction phenomena which are caused by lattice imperfections in crystals, allowed the direct observation of dislocations with high resolution and magnification.

II. SCOPE OF PROGRAM

It was proposed to study beryllium samples of different impurity content, in order to assess the effect of impurities on the ductility.

A. Polycrystalline specimens of vacuum-melted Pechiney flake beryllium were obtained from Nuclear Metals, Inc. in the form of small plates 12 x 12 mm in size or larger, and 0.5 to 1.2 mm thick, with grain sizes of 1 to 2 mm in diameter. In the process of fabrication, they had received an unknown heat treatment and some deformation by cutting and subsequent grinding. Electron microscope specimens were prepared from this material (1) "as-received", (2) after annealing at 900°C for 2 hours in a Purgon atmosphere and furnace-cooled, undeformed, (3) annealed in the same way but subsequently deformed by bending, (4) ice-water quenched from 1150°C and undeformed, and (5) ice-water quenched and deformed by bending. Spectrographic analysis indicated an impurity content in parts per million by weight as follows:

Al	80	Fe	190
Ca	< 50	Ni	190
Mg	< 50	Cr	25
Si	< 25	Mn	15
Cu	< 5		

B. Beryllium single crystals of commercial purity were available as strips, approximately 1 mm thick. The crystallographic orientation was such that the basal plane of the hexagonal unit cell formed an angle of approximately 45° with the flat surface of the specimens and was tilted around the [1100] direction.

Before investigation in the electron microscope, this material was treated in various ways: (1) annealed at 1150°C for 1 hour in a Purgon atmosphere, furnace-cooled, and deformed by compression with 50,000 and 100,000 psi,

the compression axis being perpendicular to the flat surface of the strip; (2) ice-water quenched from 1150°C, undeformed; (3) ice-water quenched from 1150°C and compressed with 70,000 psi; (4) rapidly quenched from 1150°C by means of a special apparatus to be described later, the specimen remaining undeformed; (5) rapidly quenched from 1150°C and deformed by compression with 100,000 psi; and, finally, (6) annealed at 1150°C for 1 hour, deformed by compression with 100,000 psi, and then reannealed at 800°C for 30 minutes for the purpose of polygonization studies.

These single crystals were of commercial purity, i.e., their impurity content was in the order of 0.6%, with the detailed analysis as follows (ppm by weight):

Al	970	Cr	100
Ca	< 50	Mn	95
Mg	< 5	Cu	5
Si	35	C	3000
Fe	1000	O $\sim$	600
Ni	105	N	134

The unusually high carbon content may be due to a local enrichment of C and not typical for the material as a whole.

C. Very high purity material, prepared from distilled beryllium and subsequently subjected to zone-refining, was available in the form of single crystal tensile specimens. Three specimens have been studied. Specimen 1 was machined at The Franklin Institute Laboratories from distilled beryllium which had received one fast zone-refining pass. Its basal plane and the [11$\bar{2}$0] direction formed an angle of 45° with the crystal axis. The specimen was tensile strained to fracture with a resulting elongation of approximately 35%. Specimens 2 and 3 originated from one and the same bar of distillate and were, after receiving six zone-refining passes, machined into tensile specimens by Nuclear Metals, Inc. both of their basal planes formed an angle of approximately 45° with the tensile axis, but in specimen 2 only one slip system in the basal plane was operative, i.e., the [11$\bar{2}$0] direction, on which slip occurred, was oriented 45° to the tensile axis, while in specimen 3 two slip systems were designed to operate, the respective <11$\bar{2}$0> directions symmetrically forming angles of 52°15' with the specimen axis. Specimen 2 was tensile strained 21%, while specimen 3 was elongated only 12%. Neither of the two specimens fractured during the straining.

No analytic data on the purity of these specimens was available. An indication of the purity of the materials from which specimens 2 and 3 were machined may, however, be given by the ratio of the electrical resistance at room temperature over that at 4.2°K, which was estimated to be 300-350 by Nuclear Metals, Inc., the supplier of the crystals.

2

III. TECHNIQUES OF SPECIMEN PREPARATION

The specimen holder of the electron microscope (a Philips EM 100 B was used for most of the investigations) can accommodate specimens of approximately 3 mm diameter, with a maximal thickness of 0.5 mm. The crystals to be studied had, therefore, after heat treatment and mechanical straining as required for the particular experiment, to be cut to size. For the specimens as described under Section II-A and B, electrolytic cutting techniques were used exclusively, while the tensile specimens mentioned under II-C were shaped by the spark-cutting technique with subsequent electropolishing in order to remove possible surface damage from the specimens.

One of the main problems in studying dislocations in beryllium by means of transmission electron microscopy was to find a suitable method of producing thin metal films, 1000 to 5000Å thick. Two different electrolytic polishing procedures were employed during this project, both having their own peculiar advantages and disadvantages. Reference will be made to these two procedures in the following description of the "slow" and the "fast" method.

A. The preparation of microscope specimens by the "slow" method required the material to be in the form of small strips, 3 mm wide and approximately 0.5 mm thick. The strips were cut from the little beryllium plates by means of a thin, spread-out stream of dilute HNO_3, ejected from a flat jet, and directed against the edge of the specimen, while a current of ca. 300 ma. was maintained to flow from the specimen to the jet. This permitted a fairly accurate and fast way of cutting. The beryllium strips thus obtained were subjected to the electropolishing bath (to be described) and polished down over their entire surface until their thickness was approximately 0.5 mm. The next step required the etching of a series of small, round depressions along the strip, about 4 mm distance between the depressions. This was done electrolytically by means of a fine jet stream of dilute nitric acid, directed against the surface of the strip, with a current flow of approximately 100 ma. The bottoms of the depressions were thus thinned down to about 50–100μ. The strip was now electrolytically cut into little segments, each containing one depression pit in its center. These little chips, having now roughly the size of the finished microscope specimens, were further electropolished, until a small hole broke through at the center of the depression. Around the hole a sufficiently large area was usually produced which was thin enough for electron transmission. This final electropolishing process is rather time-consuming and critical. The apparatus used for this "slow" polishing is shown in Figure 1.

The beryllium specimen, which was held in the electrolyte by aluminum tweezers (protected by Microstop lacquer), formed the anode, while a thin plate of stainless steel at the bottom of the cell served as the cathode. The cathode plate had a small hole in its center, through which a strong light beam was focused from below on the specimen. The specimen was observed constantly by means of an optical microscope of about 50X magnification, either by eye or by a photomultiplier-triggered relay circuit, until the first breakthrough of light was detected at the center of the depression. The specimen was then immediately removed from the polishing bath, washed in distilled water
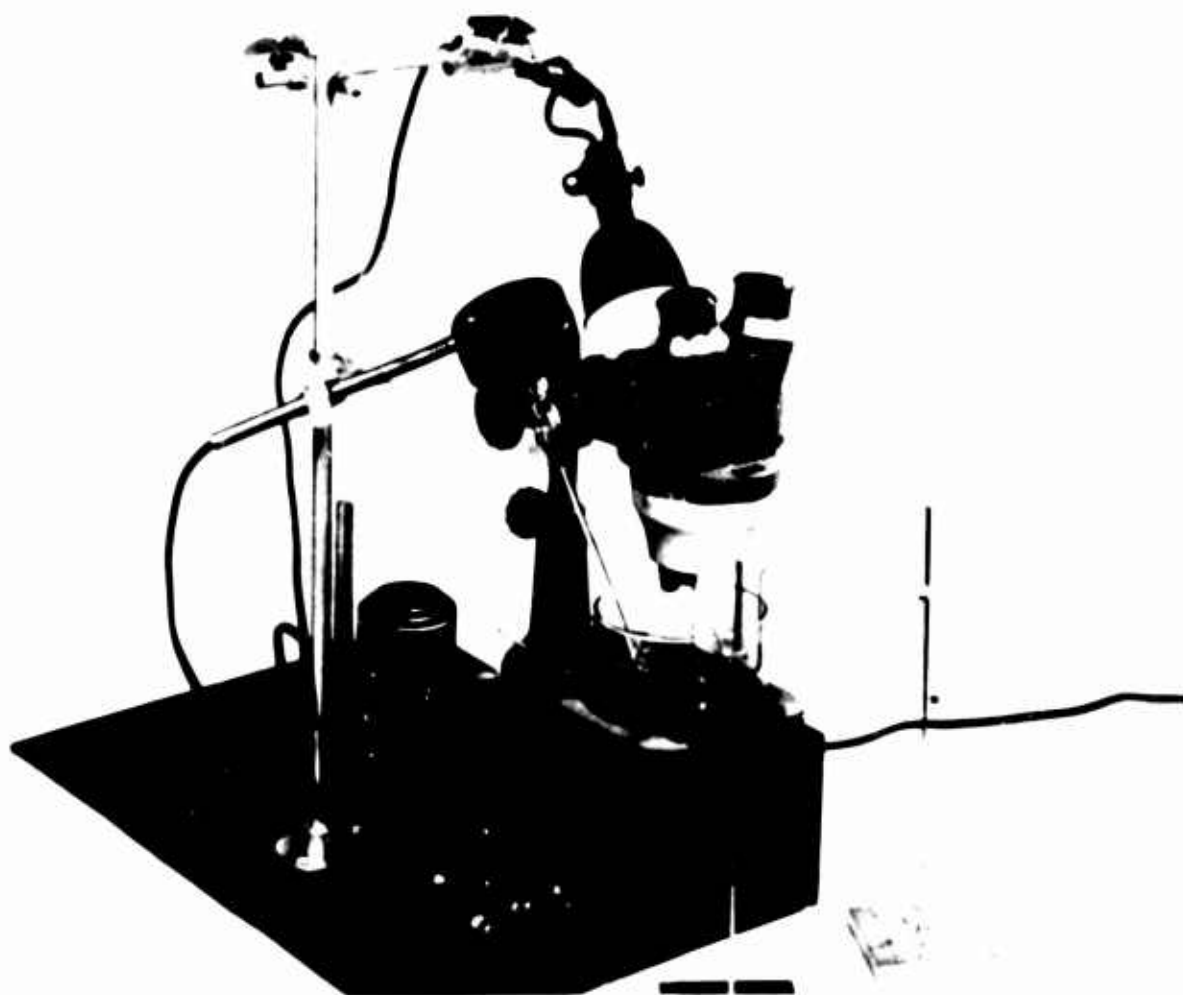
Figure 1 - Electropolishing apparatus used for the preparation of thin specimens for transmission electron microscopy. ("Slow" method).

and alcohol, and dried. The composition of the electropolishing solutions used was:

100 parts orthophosphoric acid

30 parts concentrated sulfuric acid

30 parts ethanol

30 parts glycerol

This bath was agitated and kept at room temperature. The electropolishing process was slow, reduction in thickness being approximately 4μ per hour. A voltage between 1 and 15 volts was employed, resulting in a current density of approximately 20 ma/cm^2. The current observed was remarkably independent of the cell voltage: between 2 and 20 volts the current density remained almost unchanged (Figure 2). Best polishing was obtained between 10 and 15 volts. Above 15 volts, unstable conditions occurred occasionally, resulting in a strong current surge and etching under gas evolution. At voltages near 2 volts, the gas development at the specimen (oxygen) ceased, and below 1.5 volts, hydrogen was generated. Polishing at these low voltages was poor, with etch pits becoming a serious problem. However, it has been observed that specimens prepared under hydrogen development show, when studied in the electron microscope, a clearer background than that which is usually found in specimens prepared under oxygen development. It seems that the oxygen reacts with the beryllium surface, causing a dark, spotty surface film to form. A compromise has to be made between optimum polishing conditions (negligible pitting) and a clean, smooth surface.

In work with polycrystalline beryllium, it has been noticed that the optimum polishing voltage depends also on the particular grain orientation. Slight variations in voltage cause one or the other grain to be polished, while a neighboring grain may retain its dull appearance (Figure 3). A word of caution is in order: it was frequently observed that beryllium specimens electropolished with the orthophosphoric acid solution described showed many fine dark dots, between 50 and 400Å in diameter (Figure 4). These dots were at first mistakenly interpreted as impurity precipitates within the material, until they could be identified as artefacts created at the surface of the specimens during the electropolishing procedure. Esterification and polymerization processes in the electrolyte may be responsible for the appearance of the dark dots.

B. The "fast" electropolishing method has been developed from the Knuth System of electropolishing, making use of experiences with the Disa-Electropol apparatus. With the Disa apparatus, thin polished flakes of material are obtained, floating in the electrolyte. This method is not practical for dislocation studies because thin flakes are very sensitive to deformation by handling, and the predetermined crystallographic orientation cannot be marked. Simply to exchange the slow electrolyte used in the previously described method failed to give good results. A new apparatus has been developed which combines the advantages of Disa with that of the "slow" method. Using the electrolyte E-2, as suggested by Saulnier (J. Nucl. Materials, 2, No. 4, 299-309, 1960),

5
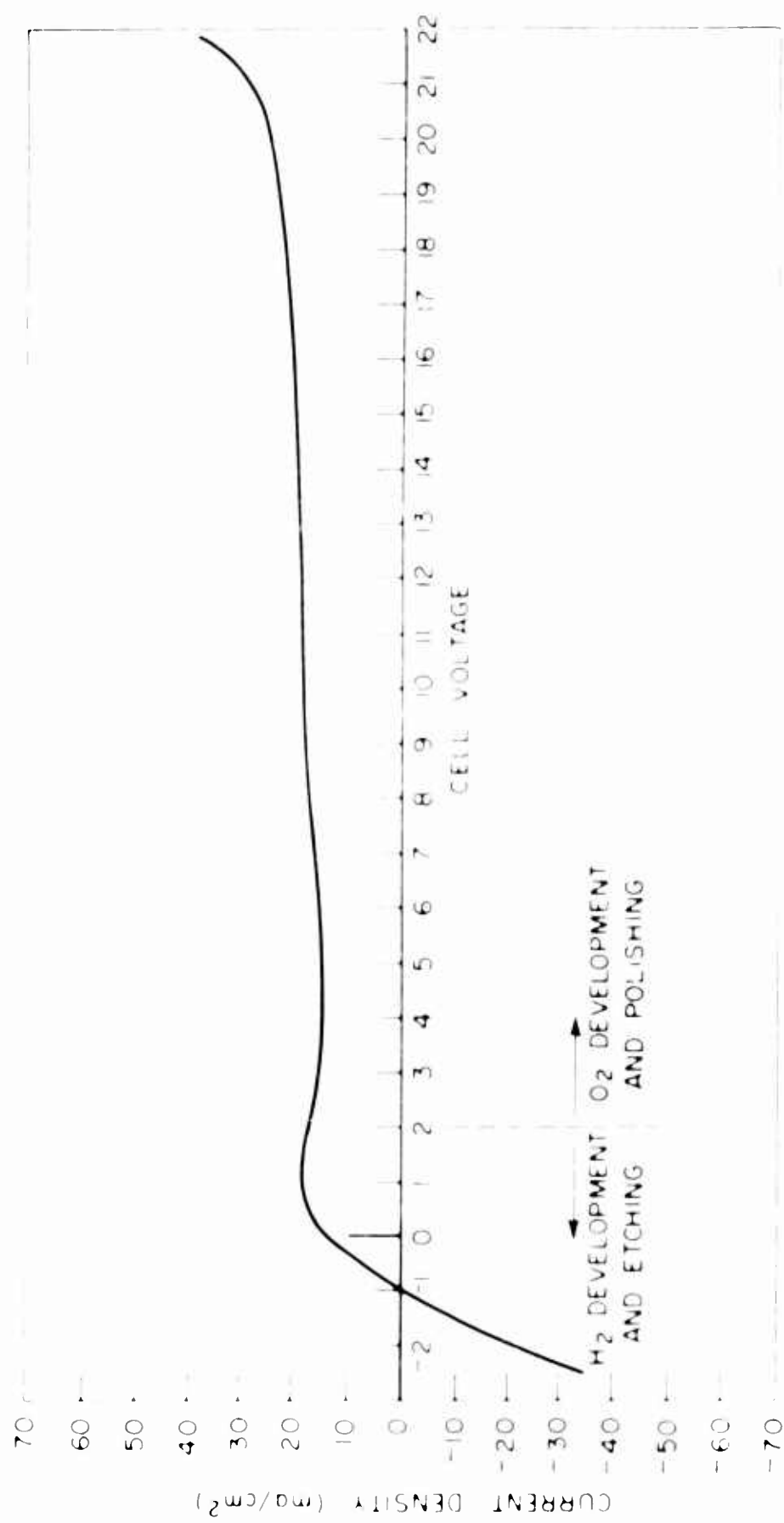
Figure 2 – Current–voltage diagram for beryllium electropolishing cell
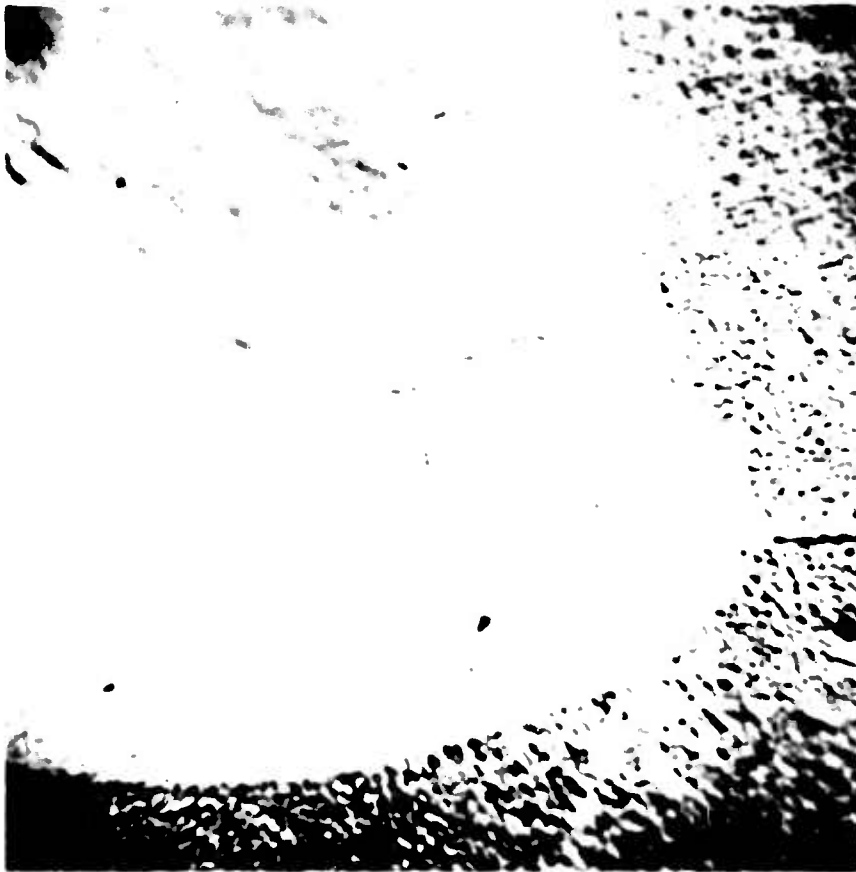
Figure 3 - Different orientations of crystal grains revealed by the
electropolishing process.   600:1.

Figure 4 - Fine dark dots, marking the surface of beryllium specimen,
are due to the electropolishing process employed. 40,000:1.

consisting of 300 parts of copper (II) nitrate, 900 parts of methanol, and 30 parts of nitric acid, much higher current densities ($\sim$80 ma/mm^2, with a potential of 50 volts across the cell) can be obtained. In the apparatus shown in Figure 5, the specimen to be polished is held by a spring against a small circular opening (about 1-2 mm dia.) in the plastic mask, thus exposing only a small section of one side of the specimen to the electrolyte. It is important to circulate the electrolyte rapidly in order to prevent changes in electrolyte concentration and an accumulation of gas bubbles at the aperture. The specimen has to be polished on two sides successively; no previous etching of depressions by means of a jet is necessary. As in the conventional "slow" method, the breakthrough of the metal film, signalizing the presence of sufficiently thin areas, is observed by an optical microscope. With this apparatus, a specimen can be polished through within a few minutes, in contrast to many hours in the "slow" method. There is a disadvantage in this faster polishing method, however. The background of the micrographs from specimens polished by the "fast" method is not as clear as that usually observed in micrographs from specimens polished by the "slow" method; it is mottled and more spotty, but dislocations come out in a clear, well-defined contrast. Both polishing methods described have as a common feature the advantage that the thin transparent film is firmly retained by a solid frame of beryllium, protecting it against accidental deformation. Both methods have been used in combination, as the conditions of the specimens demanded.

IV. THERMAL TREATMENT OF THE SPECIMENS

Annealing and ice-water quenching: wherever the experiment required heat treatment of a specimen, the specimen was first electropolished so that surface twins and other surface damage were removed that otherwise could have acted as nucleation points. After electropolishing and cleaning, the specimen was wrapped in tantalum foil and sealed in an evacuated and Purgon filled (0.2 atm.) quartz tube, 10 mm I.D. The tantalum foil was to prevent reactions between the quartz and beryllium, which may otherwise lead to a hard deposit at the surface of the specimens, making subsequent electropolishing difficult. Heat treatment proceeded as prescribed by the experiment. When annealing and furnace-cooling was called for, the quartz tube was left in the cooling furnace until room temperature was reached. Ice-water quenching was accomplished by manually pulling the quartz tube with the specimen out of the furnace at the prescribed temperature and dropping it into ice-water, immediately crushing the quartz tube in order to permit water to reach the specimen to accelerate the quenching. It is unavoidable in this method that the temperature of the specimen has dropped considerably, before it is in contact with the quenching liquid. It was therefore desirable to speed up the quenching rate. A "rapid quenching apparatus" has been built to meet this requirement (see Figures 6, 7, and 8). The beryllium specimen, about 1 x 5 x 25 mm in size, was contained in a molybdenum crucible in order to permit coupling to a radio frequency induction furnace. The crucible itself was held inside a quartz tube. The apparatus was evacuated to better than 10^{-6} mm Hg. A thermocouple permitted observation of the temperature inside

8
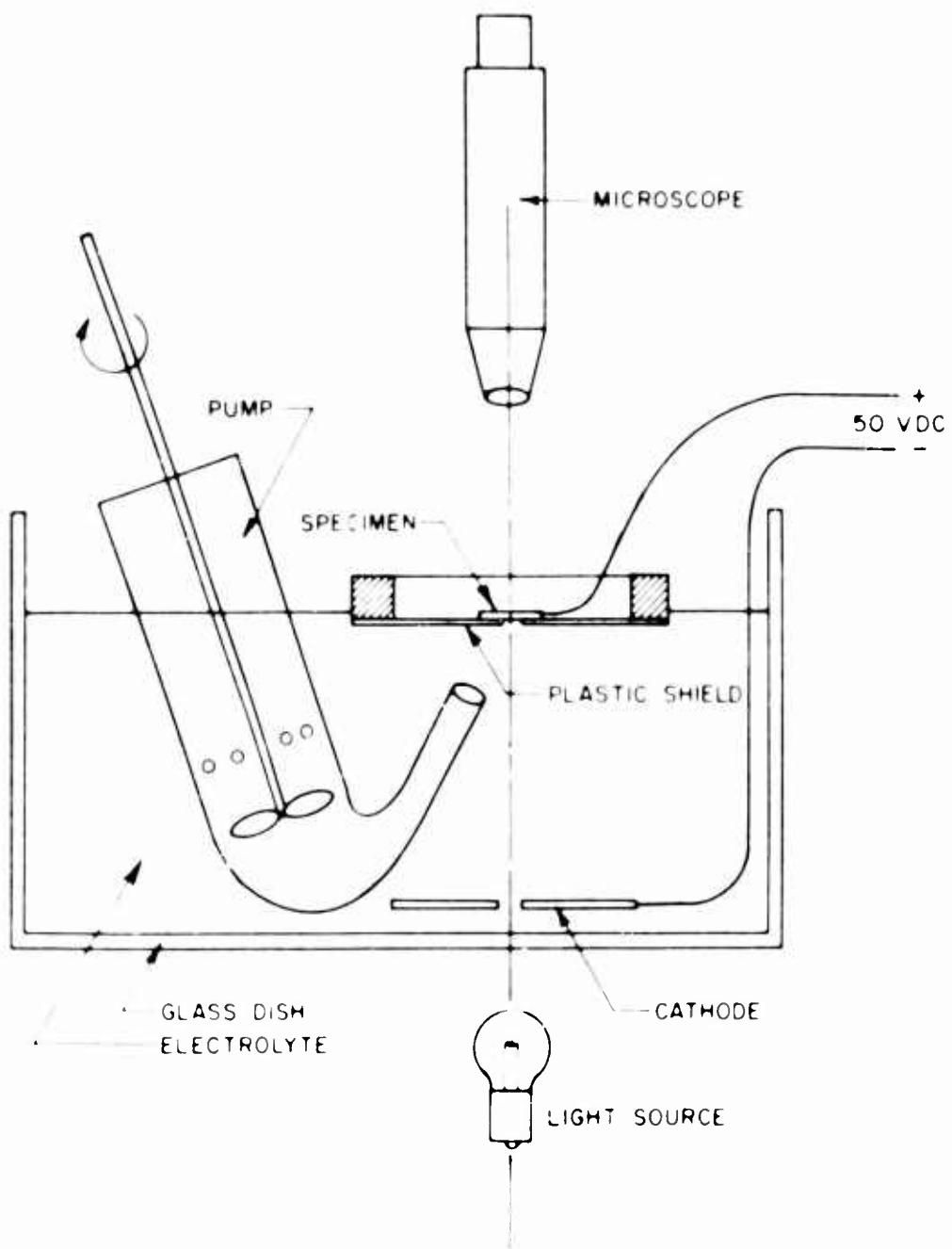
Figure 5 - Electropolishing apparatus.
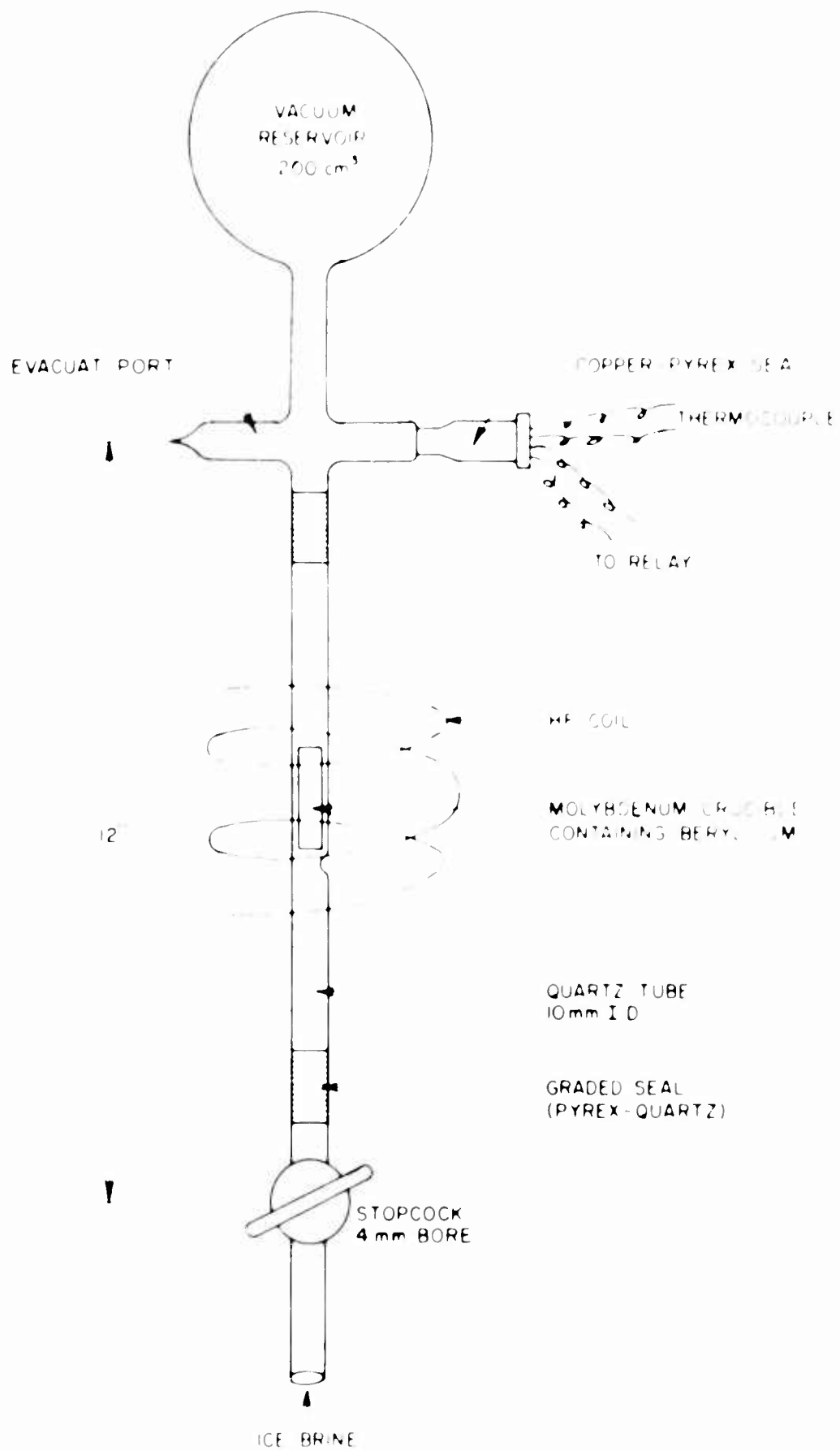
Figure 6 - Rapid-quenching apparatus.

TO RELAY

THERMOCOUPLE IN
CERAMIC TUBE

QUARTZ

MOLYBDENUM CRUCIBLE

THERMOCOUPLE

BERYLLIUM SAMPLE
(1 x 6 x 28 mm)

CONTACT FOR
AUTOMATIC
POWER CUT OFF

HOLE

SCALE 2:1
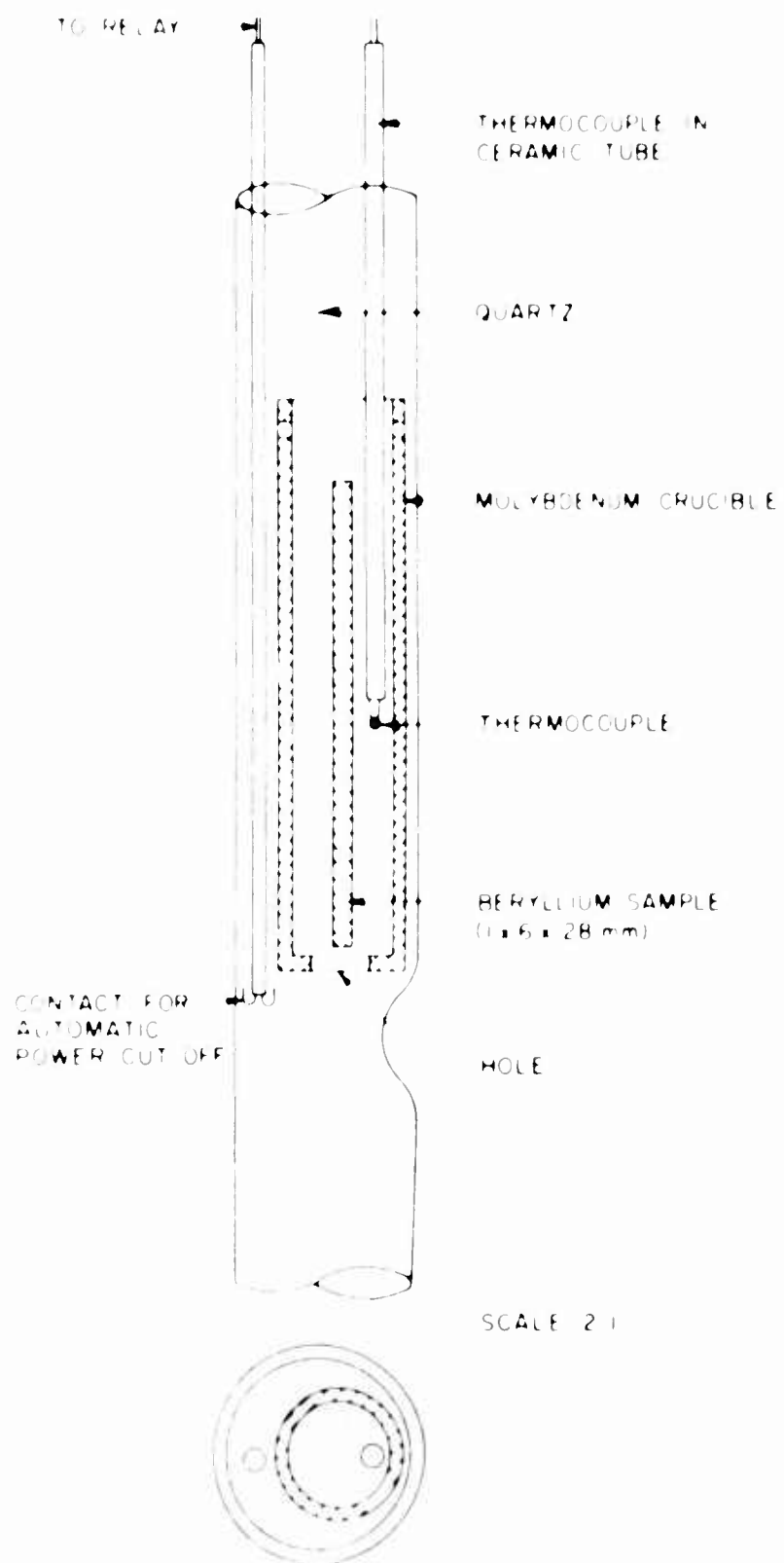
Figure 7 – Crucible with beryllium sample
in rapid-quenching apparatus.

11

TO ACTIVATING RELAY
OF INDUCTION FURNACE

FUSE

RELAY

45V

N C
RESET
SWITCH

6V

TO QUENCHING
APPARATUS
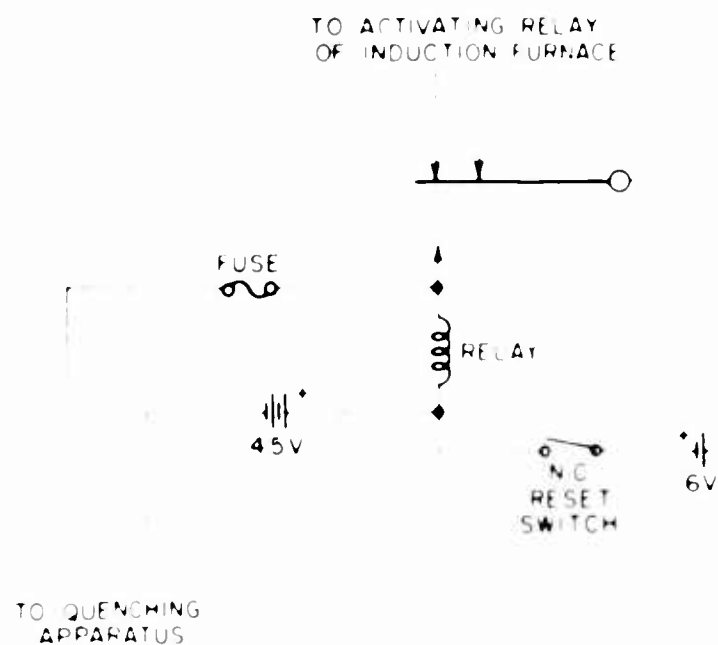
Figure 8 - Relay for rapid-quenching
apparatus (automatic power cut-off).

12

the crucible. During the experiment, the temperature was held between 1150°
and 1200°C for 30 minutes. Quenching proceeded by permitting a degassed ice
brine of -10°C temperature to rush into the apparatus while the heating power
was still on. An automatic arrangement cut the power at the moment when the
brine reached a contact point near the crucible. A hole in the bottom of the
crucible permitted easy flow of the quenching liquid through the crucible
around the small beryllium sample, thus cooling it very rapidly.

V. MECHANICAL STRAINING

Various modes of deformation were employed during this program: bending,
rolling, compression, and tensile straining. In some limited cases, while
working with polycrystalline beryllium where only qualitative information was
sought, the specimens, about 0.8 mm thick, were bent around a cylinder of 2
inches in diameter. This introduced sufficient strain to insure the presence
of dislocations, but the strain was distributed very inhomogeneously. The
specimens cracked at some places or were strongly deformed, while other sec-
tions remained practically flat.

Cold rolling of polycrystalline specimens also permitted only crude,
qualitative interpretations of the resulting dislocation patterns. An attempt
was made to tensile strain small beryllium single crystal strips of commercial
purity. These strips already showed many fine cracks along the basal plane
before straining. A specimen selected for the tensile test, apparently free
of those cracks, fractured along the basal plane at a strain of less than 0.1%.

Flat, thin single crystal strips have been deformed by compression with a
hydraulic press. The specimen was held between plain, soft iron plates, so
that the compression axis was perpendicular to the flat surface of the speci-
men. Since the crystallographic orientation of the specimens deformed in this
way was such that the basal plane formed an angle of 45° with the flat face of
the specimens, the basal plane was also inclined 45° with respect to the com-
pression axis. Compression loads of 50,000, 75,000, and 100,000 psi were used,
leading to a reduction in specimen thickness of approximately 4, 6, and 8 to 10%,
respectively.

The single crystal tensile specimens (Figure 9) of high purity (see Section
II-C) have been deformed by means of an Instron Tensile Testing Machine, with
automatic stress-strain recording. The specimen was held by especially designed
grips around its conically widened end sections, insuring proper alignment of
the crystal with the stress axis. Markings on the surface of the specimen along
its gauge length permitted, in addition, a differentiated determination of strain
along the specimen.
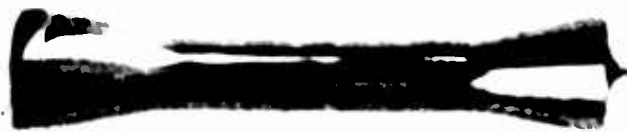
Figure 9 - High purity single crystal tensile specimen, 3:1.

VI. DISLOCATIONS IN PECHINEY FLAKE BERYLLIUM (POLYCRYSTALLINE)

The study of polycrystalline specimens of vacuum-melted Pechiney flake be-
ryllium can only be considered as a qualitative survey, but, nevertheless, it
gave important results and indications of the behavior of dislocations in be-
ryllium. Pechiney flake is of relatively high purity ($\sim$0.06% impurity con-
tent; compare Section II). From electron diffraction, etch patterns and the
length of dislocations, it is concluded that the polycrystalline specimens
studied had a somewhat preferred crystallographic orientation. The basal plane
often was approximately perpendicular to the direction of viewing.

A. Specimens as received, that were subjected to an unknown heat treat-
ment and mechanically deformed during the process of machining, revealed many
dislocations. These dislocations were, however, distributed rather unevenly
throughout the samples. Areas almost free of dislocations bordered on regions
of rather high dislocation density.

Typical micrographs of Pechiney flake, as received, are shown in Fig-
ures 10, 11, and 12. Narrow, elongated loops, a few Angstroms in width, are
seen near glide dislocations; their length varies from about 50 to 4000Å.
Further, many dark dots are noted; their diameters may be as small as 50Å or
less but were not observed larger than 200Å. One is tempted to interpret them
as impurity clusters. However, since these dots disappear as soon as the dif-
fraction conditions are not suitable for dislocation contrast, it is therefore
concluded that those black dots are small dislocation loops. Whether this phe-
nomenon is caused by vacancies, by impurities, or by both, is difficult to de-
cide on the basis of studying only these specimens. There seems to be evidence
that many dislocations are anchored (see arrow in Figure 10), and the impurity
hypothesis appears the most likely one, since some of the glide dislocations
are drawn out for large distances. It is conceivable that this strong pinning
force can be caused in various ways by an impurity cluster or precipitate. The
dislocations visible in these micrographs are predominantly straight. If
curves, they have either a large curvature (i.e., a radius of about 1 μ or
greater), or their curvature is very small (radius of a few thousand Angstroms).
Dislocation cusps, which are obviously anchored, are frequent, and their length
may reach nearly 1 μ . Most cusps, however, have a length of a few thousand
Angstroms. Sharply kinked dislocations, often in the shape of a "V", occur in
large numbers. The angle between the legs of the "V" is between 20° and 100°
of arc.

In specimens where obstacles are comparatively rare, the dislocations
have a pronounced tendency to align along crystallographic directions as deter-
mined by electron diffraction. Further, the dislocations are always immobile
at the stress created by the high intensity electron beam in the microscope.
These observations point to a high Peierls-Nabarro force in beryllium. The
dislocation structure described gives direct evidence for an extremely effec-
tive dislocation pinning. It appears that sometimes dark spots are at the
anchor points of dislocations. In this context, it is of particular signifi-
cance that most of the narrow, long loops, the "V"-shaped dislocations, and
the drawn-out cusps are pointing in the same direction.

Figure 10 - Dislocations in polycrystalline beryllium specimen (Pechiney flake, as received). Arrow indicates pinning of glide dislocation. 40,000:1.

Figure 11 - Polycrystalline Pechiney flake specimen. Many fine dots visible are recognized as dislocation loops. 40,000:1.

Figure 12 - Bundles of dislocations in polycrystalline Pechiney
flake beryllium. 40,000:1.

In previous papers, a particular type of interaction between dislocations and point defects and their aggregates, named "mushrooming", has been described (Ref. 1). This leads to dislocation tangles with interspersed prismatic loops. The Pechiney flake specimens described here exhibit such dislocation tangles with interspersed prismatic loops, in many respects so similar to those observed in f.c.c. metals that they are also believed to be the result of "mushrooming". Typical for such dislocation tangles are the long narrow loops (see Figure 11) which have previously been explained as the result of a combined glide and climb mechanism (Ref. 2). These dislocation loops in the tangles, which presumably are always at right angles to their Burgers vector, have only one direction in Figure 11. This observation seems to rule out an alternate interpretation, namely, that dislocation interactions between two systems are responsible for the tangles, and thus mushrooming remains as the most likely explanation.

The presence of long, narrow dislocation loops has been observed in recent years in a number of deformed crystals. In f.c.c. metals the loops are lying parallel to the $\langle 112 \rangle$, trailing behind screw dislocations. Their long portions, therefore, have edge character and are of opposite sign. Since various mechanisms have been proposed to explain the formation of the "dipoles", as these long narrow loops are now being called, it is of interest to study the spectrum of widths of dislocation dipoles. Some micrographs of Pechiney flake, like Figure 11, have been evaluated for this purpose and the loops countered are tabulated in the histogram, Figure 13.

To appraise this evaluation, it should be remembered that the crystallographic orientation of the individual crystal grains was not known. Some loops may therefore appear in an affine projection. This will not affect the conclusion decisively, however, because a number of very long, but extremely narrow, loops leave no doubt of their dipole character. Loops that are listed as having a width of 50Å are not resolved in the micrographs. Their widths may actually be smaller, down to atomic dimensions. They are recognized to be loops by their contrast, by their alignment with long resolved loops, and by occasional flared sections along their length. Narrow loops of extremely short extension ($< 100\text{Å}$) are not considered in this study. They may be of a different nature than longer dipoles. A small fracture of the loops counted are open loops; that means that they are actually long, drawn-out double dislocations, as for instance seen in Figure 10. They are listed as "loops" when their length-over-width ratio exceeds the value 5. The total area of the micrographs evaluated amounts to $25\mu^2$, equal to a specimen volume of $5\mu^3$. The vertical markers in the histogram represent the number of loops that were countered having a given width. To facilitate the interpretation of these values, the range of loop widths was divided into intervals of 100 Angstroms. The number of loops counted which fall into the given interval is indicated by the broken line in Figure 13. This histogram represents the density distribution of loops as a function of their widths. It is apparent that the number of loops with width $< 50\text{Å}$ increases sharply. The dislocation density in these micrographs has been measured and is found to be 3×10^9 cm/cm^3. The contribution of the narrow dislocation dipoles with widths $< 50\text{Å}$ (and lengths up to 0.6μ) to the total dislocation density amounts to $\sim 40\%$, small short-length loops (width and length $< 50\text{Å}$) contributing less than 2%.
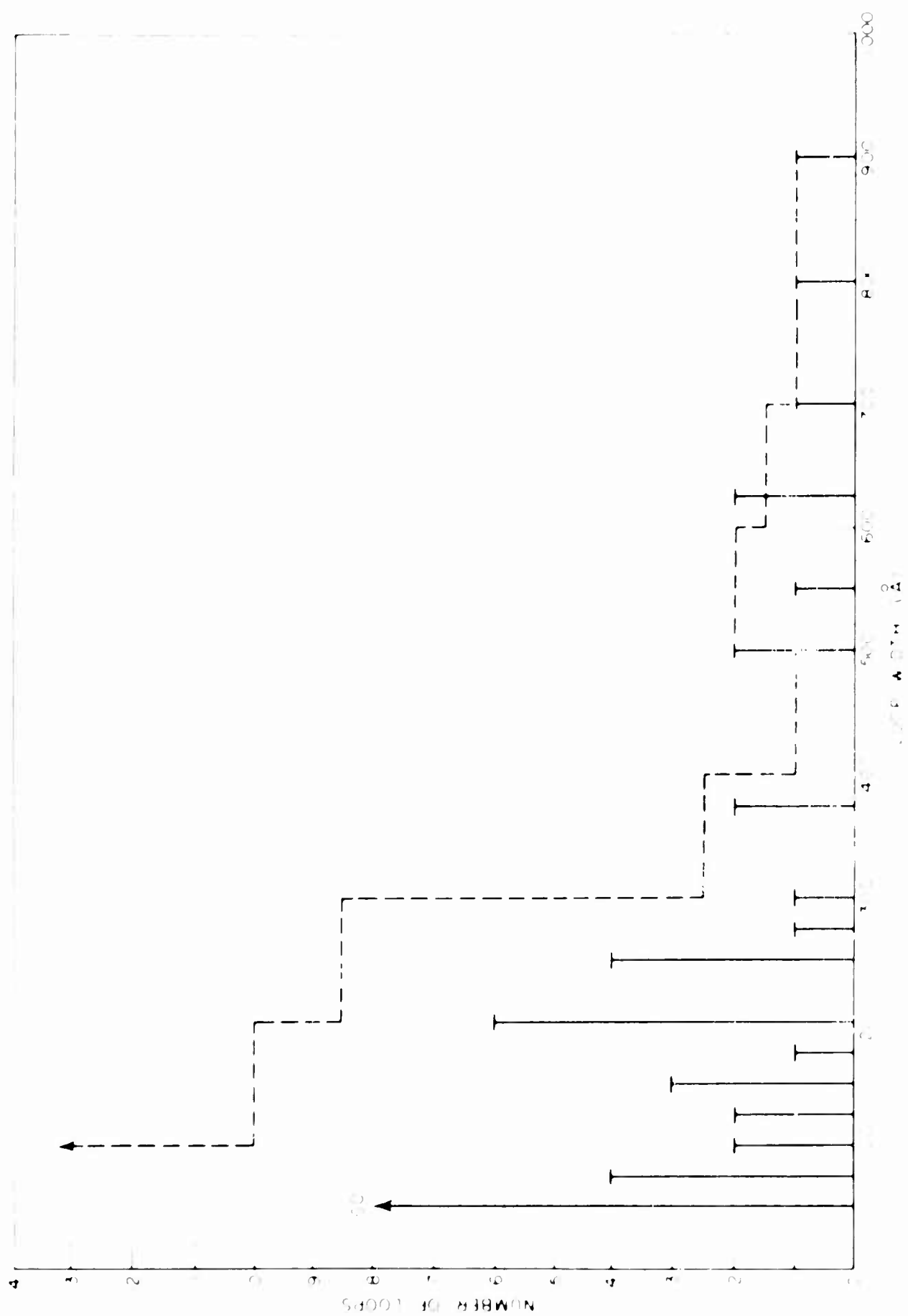
Figure 13 - Distribution of loop widths.

B. In order to study the behavior of dislocations in Pechiney flake beryllium, deformations present in the specimens when received had to be annealed out. Some electron microscope specimens were prepared from annealed and furnace-cooled material before it was strained. Very few dislocations have been seen in this unstrained beryllium. A peculiar pattern of elongated markings parallel to a certain direction was observed in many electropolished specimens, Figure 14. It is evident that these markings result from the polishing procedure. Precipitates may have formed preferably along the dislocation sites which were due to polygonization, and the electropolishing process then reveals those sites as etch pits, as shown. Some impurities, their nature not identified, were seen in similar samples. The impurities have precipitated preferably along sub-grain boundaries, Figure 15.

Annealed Pechiney flake specimens that were deformed by bending around a core of 2" diameter were electropolished and studied with an optical microscope at 270x magnification. The surface of the specimens showed many slip lines which for each grain belong to one glide system only (see Figure 16). After thinning the specimens down, the electron microscope revealed many dislocations of widely varying density. Dense bands of dislocations running nearly parallel to each other bordered on regions almost free of dislocations. Some regular dislocation networks developed. It is presumed that the dislocations in Figure 17 represent basal glide with Burgers vectors inclined 120° to each other. This could not be measured, since an electron diffraction pattern was not obtainable. On the other hand, the basal plane is the major slip plane in beryllium, and the long dislocations suggest the conclusion that the specimen has a (0001) orientation. On many intersections, no dislocation reactions seem to have taken place, but on a small fraction of intersections, the original four-fold nodes had clearly split into three-fold nodes (see arrow in Figure 17). This is of particular interest for three reasons:

(1) For metals with a low or moderate stacking fault energy, three-fold nodes should be clearly extended. No indication of extended nodes, however, was found, nor have any dislocations been seen which were split into partials. Thus, the stacking fault energy of beryllium must be high. Referring back to the discussion of dislocation tangling, it should be noted that the presence of tangles in the Pechiney flake beryllium, as received, and its absence in the specimens discussed here, rule out the explanation that the dislocation tangling is somehow dependent on the magnitude of the stacking fault energy, since there cannot be that much difference between the specimens in which evidence of tangling was present and the specimens that show dislocation networks without tangling. There are annealed specimens where irregular dislocation patterns have formed, resembling that of material "as received." The dislocation density in these specimens, however, is too low to permit conclusions concerning the likeliness of tangling at higher stresses.

(2) The observation that the dislocations shown in Figure 17 have interacted with each other proves that at least two different slip systems are involved. Nonetheless, no tangling has taken place, while the dislocations in the tangle of Figure 11 presumably belong to only one system. This is a further argument that neither the formation of intersection jogs nor dislocation interactions can be the major cause for the dislocation tangles.

20

Figure 14 - Pattern of etch pits in annealed, unstrained Pechiney flake
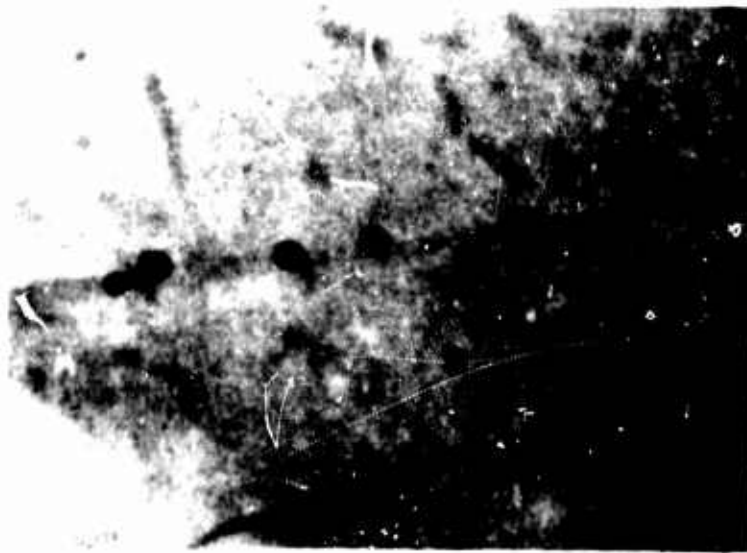beryllium. 30,000:1.

Figure 15 - A string of impurity clusters in annealed Pechiney flake
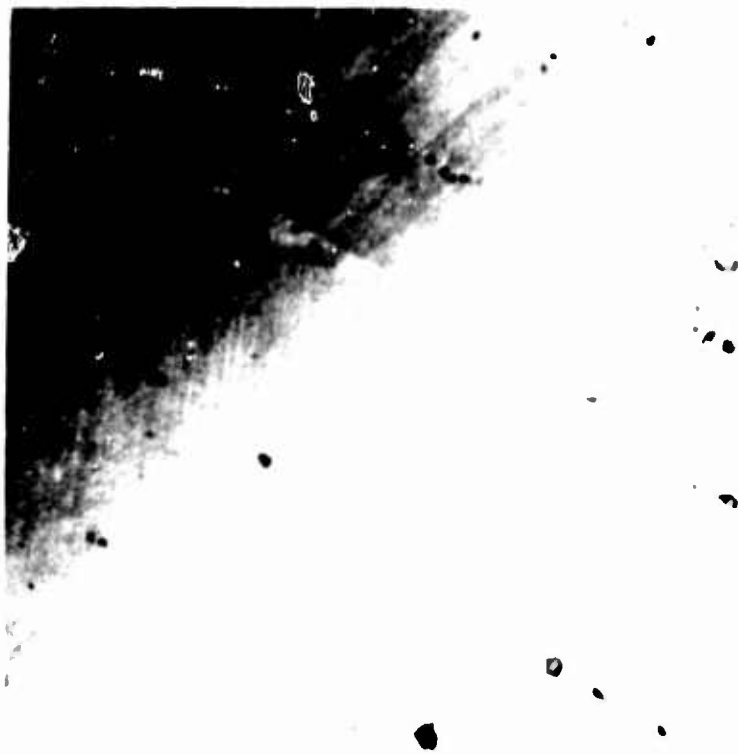beryllium. 7200:1.

Figure 16 - Slip lines in annealed and strained polycrystalline beryllium made visible through electropolishing. 270:1.

Figure 17 - Network of dislocations in bent Beckiney flake beryllium. 15,000:1. Arrow points to three-fold node discussed in text.

(3) Although a favorable dislocation reaction was clearly possible between the two systems of Figure 17, three-fold nodes have not formed at many dislocation intersections. This indicates a strong frictional stress on the dislocations, which prevents them from rotating at the four-fold nodes, presuming that the dislocations all lie in the same plane. Again, the evidence of a high Peierls-Nabarro force in beryllium is present. This should not be too surprising in the light of a recent theoretical investigation (Ref. 3).

Owing to its low c/a ratio, the basal plane in beryllium is not close-packed. Moreover, it has already been deduced that the stacking fault energy on the basal plane is high, indicating that the stacking fault position does not represent a configuration of effective minimum energy for the atoms. Consequently, the critical resolved shear stress at which slip along the basal plane would take place in the absence of dislocations must be high, and with it the Peierls-Nabarro stress.

C. Pechiney flake specimens that were underlined quenched in ice-water after being held at a temperature of 1150°C for 30 minutes also show rows of impurity clusters, sometimes along sub-boundaries. Occasionally, these sub-boundaries have been annealed out, and strings of precipitates remain in the lattice. The presence of these particles in quenched specimens would indicate that there is a considerable amount of insoluble material present. Their average diameter is approximately 500Å. The nature of the particles has not been identified. The dislocation density in these specimens is extremely low, and the dislocations form rather irregular patterns.

Anticipating a clustering of point defects at elevated temperatures, the quenched material was annealed at 300°C for two hours after deformation by bending, thinned down, and examined. Although some small loops have been seen, the results are not conclusive since they occurred together with irregular arrays of dislocations. No evidence of polygonization is present. In the micrograph, Figure 18, an avalanche of dislocations originated obviously from the large precipitate particle.

Surface investigation on specimens prepared from vacuum melted Pechiney flake material that was quenched from 1150°C, strained by bending, and polished electrolytically revealed some unusual effects. Figure 19 shows an area covered with a series of fine straight lines approximately 0.1 mm long and pointing in 3 or 4 preferred directions. These markings were seen over large surface areas, and it is not unlikely that they represent deformation twins.

VII. DISLOCATIONS IN BERYLLIUM OF COMMERCIAL PURITY (SINGLE CRYSTALS)

The crystallographic orientation of the single crystals that were studied is shown in the stereographic projection, Figure 20. The pole of the flat specimen surface is marked "A". An impurity content approximately 10 times higher ($\sim 0.6\%$) than that of Pechiney flake beryllium is found in these crystals.

Figure 18 - A larger inclusion particle acting as dislocation source.
(Pechiney flake beryllium). 40,000:1.

Figure 19 - Deformation twins in quenched and strained Pechiney flake beryllium. 325:1.
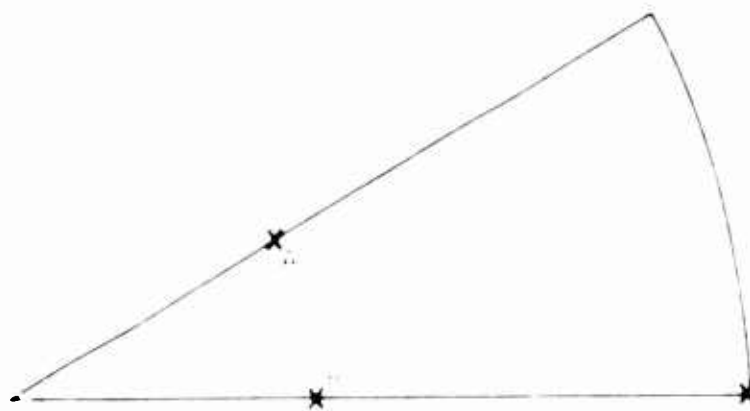
A — [illegible] ... single crystal specimens described in section XII.

△ — [illegible] ... the tensile axis of high purity tensile specimen ... and [illegible] see section XIII.

+ — Marking the tensile axis of high purity tensile specimen A described in section XIII.

Figure 20 - Stereographic Projection

(Indicating the Orientation of Beryllium
Single Crystals Used in This Study)

It has been mentioned already (Section III-A) that a remarkably uniform
distribution of fine dots seen in electron microscope specimens of this mate-
rial - annealed as well as quenched - has been identified as artefacts, due to
the polishing technique employed. Nevertheless, numerous observations of im-
purity particles have been made in beryllium of commercial purity, while such
particles are rarely seen in Pechiney flake. Inclusions, opaque to the electron
beam and as large as $2\,\mu$ in diameter, have been detected in thinned specimens,
thus verifying observations of other workers. Figure 21 shows a series of par-
ticles with diameters ranging from 0.1 to $0.25\,\mu$, as seen in quenched beryl-
lium (commercial purity). The shape of the inclusion particles is usually
round, although larger ones tend to be irregular. A few particles with regular
quadratic shape have also been found. Dislocations may sometimes be anchored
and locked in place by particles that are large enough to be clearly visible,
as shown in Figure 22.

Dislocation patterns appear quite similar in annealed and quenched speci-
mens when studied superficially. As a rule, areas of dislocations in irregular,
tangled patterns with sharp kinks and occasionally long straight sections are
found in all specimens. Closer inspection, however, reveals some significant
differences.

A. In annealed and furnace-cooled crystals that were deformed by compres-
sion, a dislocation structure as shown in Figure 23 is sometimes found. The
basal plane is tilted 45° around the $[1\bar{1}00]$ direction. Under those conditions,
single slip on the basal plane with the Burgers vector $1/2\ [11\bar{2}0]$ is expected.

26

Figure 21 - Inclusions in beryllium crystals of commercial purity.
Diameters range from 0.1 to 0.25 μ . 40,000:1.

Figure 22 - Dislocations pinned by small inclusion particles in
beryllium of commercial purity. 40,000:1.

The majority of the single dislocations visible in Figure 23 presumably belong to this slip system. Surprisingly, a dislocation array of high density in $(2\bar{1}\bar{1}0)$ is also observed. The appearance of this structure would suggest that some unpredicted slip, also on the basal plane but with $b_2 = 1/2\ [\bar{1}\bar{2}10]$, has taken place and that dislocations of these two systems meeting in $(2\bar{1}\bar{1}0)$ have reacted as $1/2\ [11\bar{2}0] + 1/2\ [\bar{1}\bar{2}10] = 1/2\ [2\bar{1}\bar{1}0]$ to form a wall of edge dislocations. This dislocation wall represents a strong obstacle against further slip on the primary slip system.

Since the specimens were deformed with a compressional force normal to their own plane, $(2\bar{1}\bar{1}0)$ is a likely fracture plane. It is tempting to speculate that the high density dislocation array in Figure 23 represents an incipient crack in that same plane. On the other hand, the dislocation array in $(2\bar{1}\bar{1}0)$ constitutes a "bend-plane" (Ref. 4), the occurrence of which has been assumed to be necessary for the formation of cracks on (0001). The condensation of edge dislocations into walls of the same nature has been frequently observed in this material as well as in Pechiney flake specimens (Figure 12). They are found to be much more pronounced in high purity specimens that were tensile-strained, as described in Section VIII.

The dislocation structure in Figure 24, also found in an annealed and compressed crystal, appears to be similar but may, however, be of a different nature. The difference in dislocation contrast on both sides of the wall indicates that the crystallographic misalignment across the wall is stronger than was found in the micrograph, Figure 23. Slight tilting of the specimen in the electron microscope increases the contrast of the barely visible dislocations, while the dislocation contrast on the other side of the wall will fade out. No such pronounced angular difference has been observed in the "bend plane" dislocation wall described above. Therefore, Figure 24 most likely shows a subboundary.

It is difficult to enumerate all dislocation observations made in annealed and deformed crystals. There are sections revealing long strands of almost parallel dislocations, observations of incipient networks, and many cases of no apparent regularity in the dislocation structure. The dislocation density is very inhomogeneous throughout, at low as well as high deformation stresses. In specimens where a high dislocation density is found, tangles are usually present. Small loops, sometimes of irregular shape, are seen whenever irregular dislocation structures are encountered. Figure 25, taken from a specimen of a series deformed by compression about 8%, has a measured dislocation density of $7 \times 10^9\ cm/cm^3$. Many dislocations lying in zig-zag formation indicate a complex deformation mechanism; their three dimensional arrangement could not be concluded from this micrograph.

During the electron microscopic investigation of these crystals, one of the few rare cases of a dislocation moving in the electron beam was noticed.

B. In order to investigate the possible influence of vacancies on the dislocation behavior, specimens of the same purity and orientation were quenched and deformed by compression. In specimens that were quenched manually from 1150°C in ice-water and deformed, dislocations due to the quenching strain as well as those due to mechanical deformation were present. Quenching dislocations are usually found to lie in the basal plane in the $[11\bar{2}0]$ direction,

28
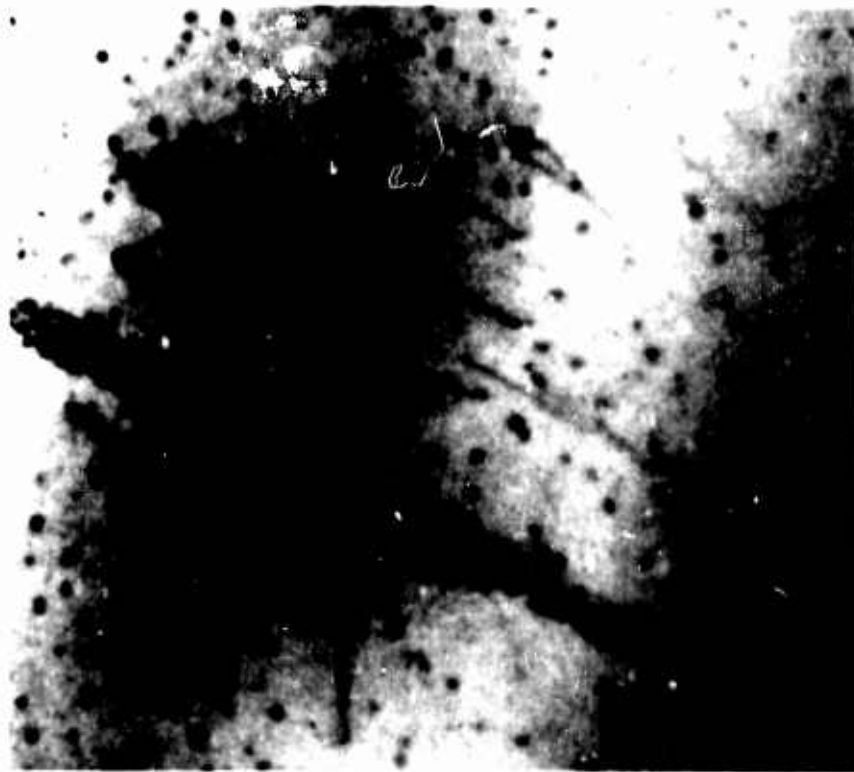
Figure 23 - Dislocation wall lying in a (2$\bar{1}\bar{1}$0) plane. Specimen was annealed, furnace-cooled, and deformed by compression. 40,000:1.

Figure 24 - Dislocation wall in an annealed and compressed beryllium crystal of commercial purity, representing a sub-boundary. 40,000:1.

Figure 25 - Dislocation pattern of high density (ca. 7×10^9 cn/cm^3) in an annealed and compressed beryllium single crystal. Deformation of sample was 8%. 40,000:1.

perpendicular to the axis of the basal plane tilt. Quite often, they reveal a slight waviness or even spiral character, as seen in Figure 26. These discontinuities are not due to a diffraction phenomenon but are real, as already noted in Section VI-C. In Figure 26, both types of dislocations are present, interspersed with particle inclusions. Dislocations due to quenching strain are found to be much more numerous when the quenching is rapid, as done with the quenching apparatus described in Section IV. Such dislocations are seen in micrograph Figure 27, taken from a rapidly quenched, undeformed crystal. Among the more complex dislocations (still in the general $[11\bar{2}0]$ direction), small loops are occasionally found.

Rapidly quenched crystals have been deformed as usual by compression with a load of 100,000 psi, the compression axis being at an angle of 45° with the $[11\bar{2}0]$ direction in the basal plane of the crystal, resulting in a relative reduction in specimen thickness of approximately 10%.

Striking is the high number of rather large, irregular loops and spiral-shaped dislocations, with winding diameters of 0.2µ and larger, that were found in thinned down specimens (Figure 28). Smaller loops, down to 100 or even 50Å in diameter are in evidence. One specimen of the same orientation, receiving the same treatment, revealed a rather dense network of dislocations. The directions of the two sets of dislocations creating this network form an angle of 60° with each other. Areas with regular networks border on regions with more irregular dislocation arrays, interspersed with loops.

Heavy deformation resulted in local lattice tilts and lattice rotations in some areas in the specimens. They were noticed as defined regions, about 1µ in diameter, that changed contrast with respect to the lattice matrix when the specimen was rotated in the electron beam. These regions were bordered by areas of high dislocation density, Figure 29.

From micrographs of very thin specimens, it was concluded on the basis of dislocation contrast with respect to extinction contours that approximately equal numbers of dislocations with positive and negative signs are present in these specimens.

Some auxiliary studies have been conducted on the formation of polygonization networks. Annealed single crystals of commercial purity, about 0.8 mm thick, with the basal plane inclined 45° with respect to the flat surface of the specimens, were compressed with a load of 100,000 psi. They were then wrapped in tantalum foil and sealed into a quartz tube with a Purgon atmosphere. The tube was held at a temperature of 800°C for 30 minutes to obtain polygonization, and then cooled in air.

As expected, hexagonal networks have been observed, with hexagon diameters varying from 180 - 4000Å (Ref. 5). A survey of the micrographs obtained gives no indication of open nodes at the cross points of the networks. Dislocation groupings forming tilt boundaries were also observed (see Figure 30).

Some surface observations on crystals of commercial purity are worth noticing. Crystals deformed by compression regularly showed bands of slip lines

31
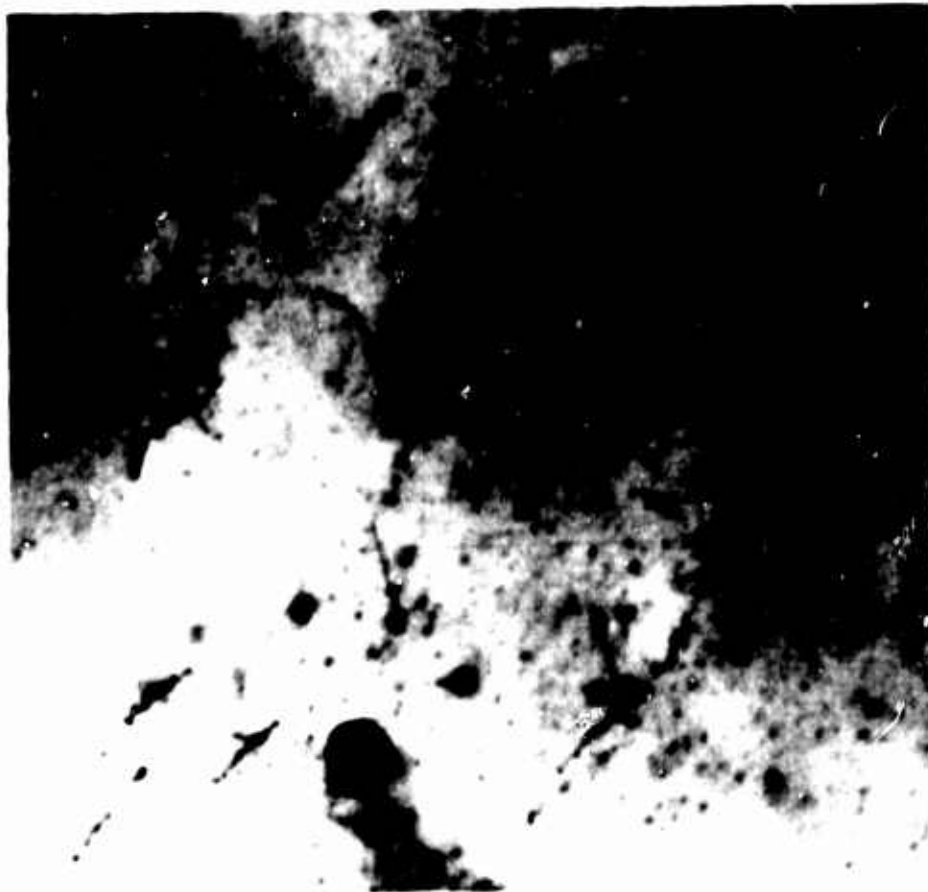
Figure 26 - Dislocations due to quenching and mechanical deformation
in commercial purity beryllium. Specimen was manually
quenched in ice-water. 40,000:1.
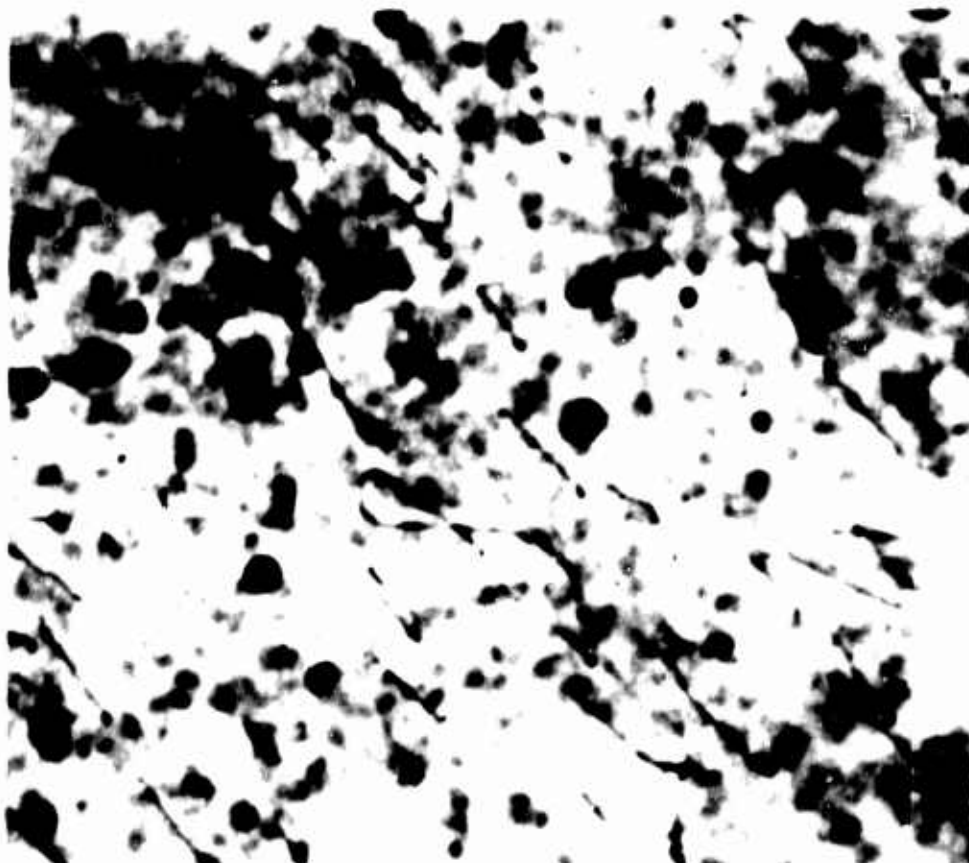
Figure 27 - Dislocations in an undeformed crystal subjected to rapid
quenching. 4,000:1.

Figure 23 - Rapidly quenched crystal of commercial purity, deformed by compression ca. 10%. Note large irregular dislocation loops and spiral-shaped dislocations. 40,000:1.

Figure 29 – Heavy lattice deformation in a quenched and deformed beryllium crystal. 40,000:1.

Figure 30 - Hexagonal dislocation network due to polygonization in a single crystal that was deformed by compression and re-annealed at 800°C for 30 minutes. 40,000:1.

after electropolishing, when investigated under the optical microscope. In a specimen where tensile straining had been attempted, these slip bands were confined to the immediate fracture zone (fracture occurred here along the basal plane with less than 0.1% strain accomplished). The surface of cold rolled crystals was to about 30% marked with twins after polishing. Many fewer twins were found in crystals deformed by compression.

A single crystal of a different orientation, the basal plane perpendicular to the flat surface of the specimen, was annealed at 1150°C for one hour and allowed to cool in the furnace. After electropolishing, the specimen was investigated with an optical microscope. A substructure similar to that observed frequently in zinc was found (see Figure 31). A network of elongated cells is formed, with the basal plane trace in the direction of the longer cell dimensions. Undoubtedly, these cell boundaries are due to a concentration of impurities (probably aluminum or iron) produced during the solidification and annealing process. Similar observations have been made on zinc where this phenomenon has been extensively studied (Ref. 6).

VIII. DISLOCATIONS IN HIGH PURITY BERYLLIUM (SINGLE CRYSTALS)

A. Specimen 1: A single cry. 1 tensile specimen was made available for electron microscopic studies after it had been tensile strained in The Metallurgical Laboratory of The Franklin Institute. It was spark machined from vacuum-distilled beryllium (supplied by Nuclear Metals, Inc.) after receiving one fast zone-refining pass. Its basal plane and [11$\bar{2}$0] direction previous to straining were inclined 45° to the specimen axis. The specimen was strained to fracture, which occurred along the basal plane. Its elongation amounted to 32.3%. Figure 32 shows a micrograph characteristic for the fracture surface. Microscope specimens were cut from this crystal parallel to the basal plane by electrolytic techniques. The first specimen of this series was taken from the section adjacent to the fracture plane, its polished thin area approximately 30 μ distant from this plane. Other specimens, cut from sections farther down in the crystal, revealed, however, the same details.

Very characteristic are dense bundles of dislocations, their direction being parallel to (11$\bar{2}$0) planes and perpendicular to the direction of slip (Figures 33 and 34), thus identifying them as being composed of edge dislocations. The length of these bundles ranges from approximately 1 to 10μ, with an average length of 5μ. Their width is approximately 800Å. About four bundles were counted within an area of 100μ^2. The dislocation density within the bundles is high. Assuming a thickness of 2500Å for the specimens, the maximum observable dislocation density is calculated to be 10^{11} cm/cm^3. This density is exceeded within the bundles. Occasionally, it can be observed that the contrast of the dark bundles changes to a very light contrast when the specimen is tilted slightly in the electron microscope, indicating a large amount of shear within the bundles. Typical dislocation densities between the bundles range from 6-11 x 10^9 cm/cm^3. Making use of the formula $\gamma = \rho b \ell$, the average travel length ℓ for dislocations can be calculated. ρ is the dislocation density, $\bar{b}$

Figure 31 - Substructure in annealed beryllium single crystal of commercial purity. Cell boundaries are due to a concentration of impurities. 350:1.
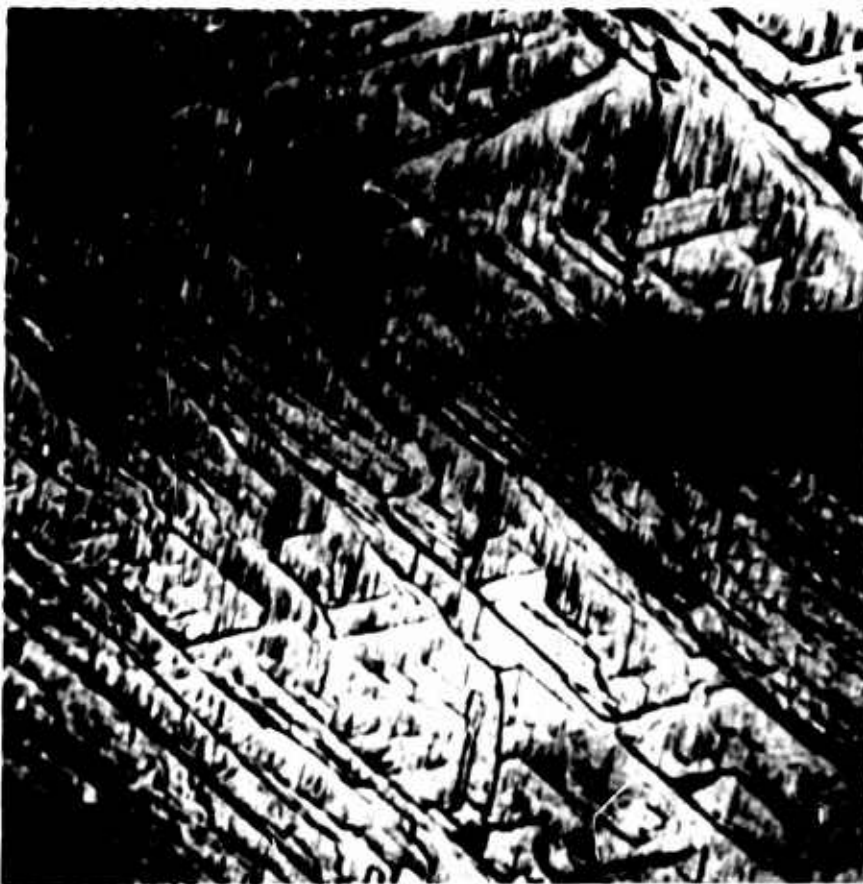

Figure 32 - Fracture surface on beryllium tensile specimen. 300:1.
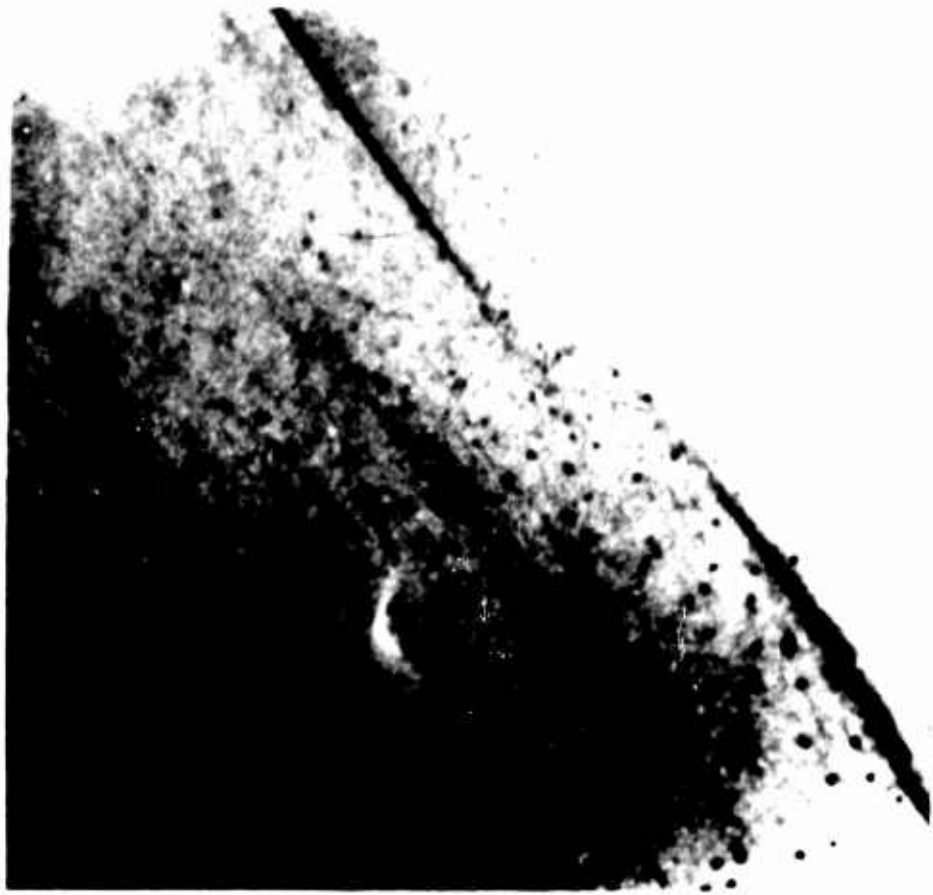
Figure 33 - Dense bundles of dislocations in a high purity beryllium
tensile specimen, lying in the basal plane parallel to
(1120). 12,500:1.

Figure 34 - Long straight and kinked dislocations between dense
dislocation bundles. 40,000:1.

the Burgers vector, and γ the resolved shear strain. With a specimen thickness of 2500Å and a density of 10^{10} cm/cm^3, a dislocation travel length of 30μ is calculated.

A striking similarity is noticed between the dislocation bundles described here and the dislocation wall shown in Figure 23. Note that the dislocations between the bundles in Figure 34 are much longer than those in Figure 23, because the basal plane is viewed perpendicularly in Figure 34, while it appears under an angle of 45° in the micrograph in Figure 23. Sharp kinks, as have been observed in other samples of different treatment, are again present in addition to dipoles or long loops. Sometimes, more or less regular networks are formed, for which Figure 35 gives an example. A larger precipitate particle acting as a source for dislocation loops, spread out in the direction of slip, is seen in Figure 36. Observations on this specimen have been verified by a comprehensive study of specimens 2 and 3.

B. Specimens 2 and 3, mentioned in Section II-C of this report, were obtained from the center of a bar which was subjected to six zone-refining passes. The zone-refined bar was made from distilled beryllium. After spark-machining, the tensile specimens were electropolished, removing an additional 5 mils from the surface of the specimens. An indication of the purity of the material may be given by the estimated resistance ratio

$$\frac{R_{RT}}{R_{4.2°K}} = 300 - 350$$

This estimate was made by Nuclear Metals, Inc., who supplied the tensile specimens 2 and 3.

Specimen 2 appeared to be slightly bent when received. Optical microscopic inspection of the surface revealed clear traces of intersections of basal plane with the cylindrical surface over its entire length. This cannot be taken as evidence that the specimen had been deformed accidentally, since polishing may produce this effect also. Some small etch pits observed were considered insignificant for the following studies. The crystallographic orientation was determined by a Laue back-reflection. The basal plane was found to form an angle of 39° with the axis of the specimen, tilted around the [1̄100] direction, so that only one glide system [112̄0] was expected to be operative in the tensile test. The overall length of the specimen was slightly less than 1 inch, with about 12 mm gauge length. The thickness varied along the gauge length of the specimen from 2.62 mm diameter to 2.72 mm, with an average diameter of 2.65 mm. During the tensile test, a strain of 21% (measured between two gauge marks) was obtained. The strain along the specimen was, however, not uniform, ranging from 2% at one end to almost 32% near the center part. The specimen did not fracture during the test. A maximum stress of 2.47 kg/mm^2 (3530 psi) was measured. After the tensile deformation, the new orientation of the basal plane was determined. It was now found to include an angle of 30° with the specimen axis in regions of heavier deformation, and 37°
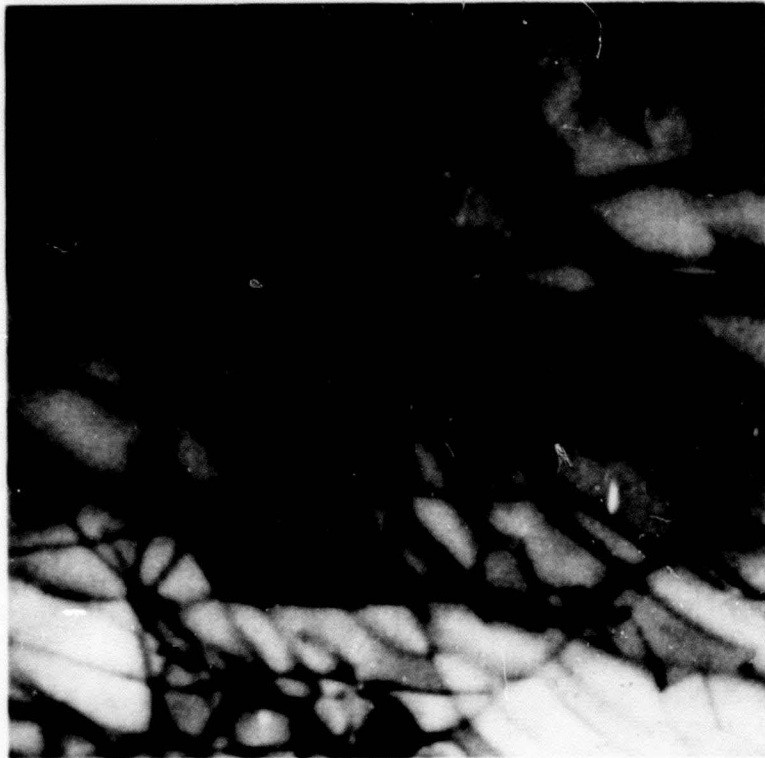
Figure 35 - Dislocation network found between dense dislocation bundles. 90,000:1.
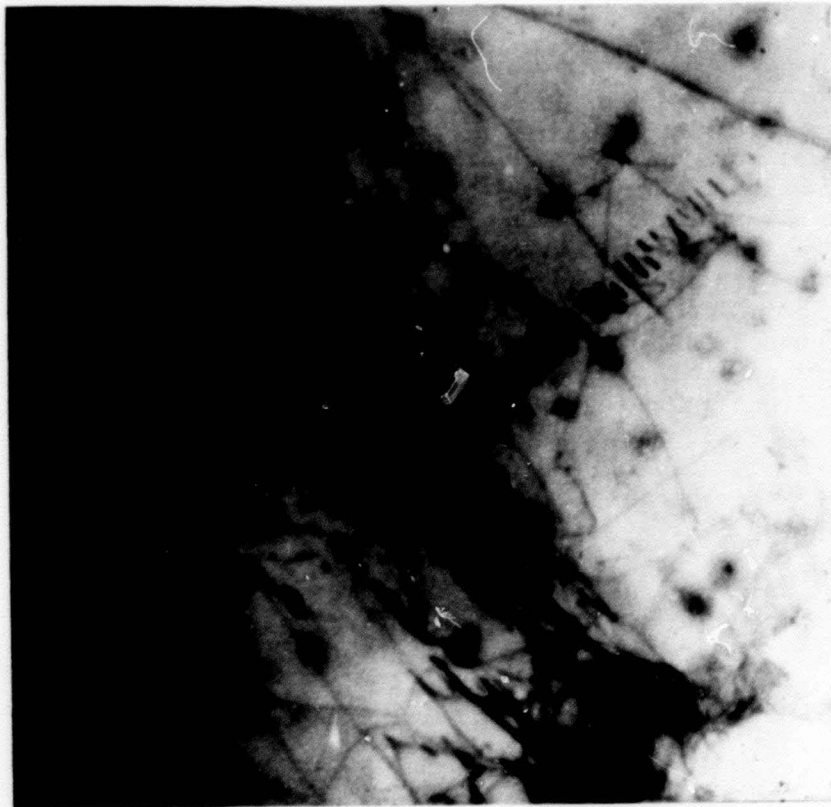

Figure 36 - A precipitate particle acting as source for dislocation loops in a high purity tensile specimen. 40,000:1.

in regions where the deformation was slight. Slip lines with clearly discernible steps were visible in the optical microscope. Only basal plane slip could be detected in this way.

In order to prepare electron microscope specimens, thin slices (0.5 mm thick) have been cut from the crystal parallel to the (0001) basal plane, and others parallel to the (10$\bar{1}$0) prism plane that was subjected to maximal strain. Cutting was done by means of a spark cutting machine. Transmission specimens for electron microscopic investigation have been prepared from the center of the slices, thus polishing off any possible surface damage done during the cutting. It was noticed that frequently cracks opened up in the samples during the polishing process, running parallel to the basal plane. In fact, specimens cut parallel to (10$\bar{1}$0) fractured very easily along the basal plane, even with no apparent stress applied.

The dislocation pattern of microscope specimens cut parallel to the (0001) basal plane from this sample resembles closely that of specimen 1. Long drawn out arrays of edge dislocations and a large number of dipoles and long loops were observed, their long portions likewise having edge character. Dislocation bundles were formed of a high density, as have been observed in specimen 1, as well as bundles that were formed in a more loose fashion, shown in Figure 37.

A characteristic pattern of kinked edge dislocations, their kinks connected by screw dislocations, is shown in Figure 38. It has also been observed in the diffraction electron microscopy of zinc (Ref. 7). Most striking, however, is the formation of long dipoles (see Figure 39). That their long sections are edge dislocations of opposite sign is concluded from their direction at 90° to the main slip system and the change of contrast between their components. The stable position for parallel edge dislocations of opposite sign is, because of the hexagonal anisotropy, slightly different from 45°. It is calculated to be 46°5' as measured from the basal plane (Ref. 8). It is safe to assume then (and this view is supported by micrographs of the (10$\bar{1}$0) prism plane) that the components of the dipoles observed lie in basal planes separated by approximately 250Å, i.e., under an angle of 46° to the [11$\bar{2}$0] direction in the basal plane.

The forces between the parallel dipole sections have been calculated. The force component in the basal plane for the stable configuration is zero, while the force component perpendicular to the basal plane amounts to an attraction of 4.8×10^{-3} dyne/μ . This value is based on the elastic constants of beryllium as measured in 1956. It may be in error to the extent that the elastic constants of the material investigated here are different from those of beryllium available some years ago.

The dipoles appear to be twisted at some points, and interactions with dislocations, possibly belonging to another glide system, are visible. Many dislocations are lying in $\langle 1\bar{1}00 \rangle$ directions, having $\langle 11\bar{2}0 \rangle$ Burgers vectors. The angles between kinked dislocation sections quite frequently measure 60° or 120°, respectively. It should be remembered that dislocations lying in the prism plane, if present, could not be seen in these specimens, since they are cut perpendicular to the (1$\bar{1}$00) plane. It is likely that the zig-zag dislocation shown in Figure 39 is part of a screw dislocation, anchored at the kinks by lattice imperfections.

Figure 37 - Dislocation bundle composed of a less dense array of
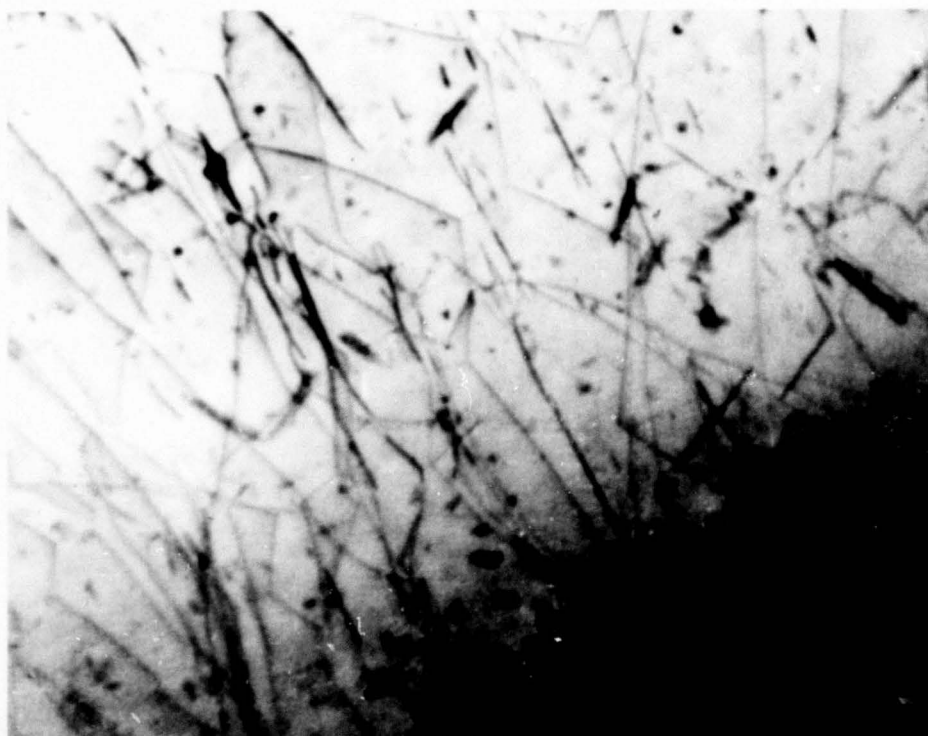edge dislocations. 40,000:1.

Figure 38 - Dislocation pattern in high purity beryllium tensile speci-
men. Note several barely visible dislocations joining kinks
of two neighboring edge dislocations. 40,000:1.

Figure 39 - Dipole formations in a high purity beryllium crystal.
40,000:1.

Figure 40 is a micrograph of a specimen cut parallel to the prism plane $(10\overline{1}0)$, as indicated by its pole, marked "C" in the stereographic projection, Figure 20. The glide packet traces shown mark the basal plane. No other dislocation, justifying the assumption of slip on prism planes, could be detected. Quite frequently, the glide packets reveal long dislocations with dipole character, the projected distance of the dipole components being in the order of 250Å. They may therefore be perpendicular projections of dipoles as shown in Figure 39. Thicker glide packets up to 4000Å are present. Occasionally, strands of packets even as wide as 1μ were seen. An average distance between neighboring glide packets is 1.5μ. The assumption that the majority of dislocations are concentrated in the thin glide packets would give travel lengths for the dislocations even greater than previously calculated (a value of 30μ had been calculated under the assumption of uniform dislocation density).

Specimen 3, identical in purity with specimen 2, was of comparable length. Its diameter was smaller, ranging from 1.94 mm to 2.18 mm. The basal plane was found to form an angle of 45° with the specimen axis, the two $\langle11\overline{2}0\rangle$ directions on which glide was expected to occur lying with 3° accuracy symmetrical to the axis. The tensile axis of this specimen is marked "B" in Figure 20. A series of cracks was seen at one end of the specimen near the grip section, the cracks following the outline of the basal plane traces, Figure 41. However, when strained, no fracture occurred. Practically no elongation was measured in the region of the cracks, but they could optically be seen to have slightly widened. Maximum strain at one section along the crystal was near 28%; overall strain between gauge marks was 12%. The study of the surface after straining again revealed slip lines. It is interesting to note that the rather weak slip lines near the cracks (low deformation) do not follow exactly the direction of the cracks. The slip lines in most regions of the crystal were rather straight, marking the basal plane. In one small region, double slip was found to be present, owing to glide on both the basal plane and a prism plane (Figure 42). The oblique angles in Figure 42 are due to the fact that the $(10\overline{1}0)$ plane on which the double slip was observed is seen under an angle, and the slip traces are projected on a cylindrical surface.

Electron microscope specimens were cut from this crystal again parallel to the (0001) basal plane and parallel to a $\{10\overline{1}0\}$ plane on which double slip had been observed.

In micrographs viewing the $(10\overline{1}0)$ prism plane perpendicularly, no significant difference was detected when compared with similar micrographs of specimen 2, in which only one slip system was operative. Thick glide packets were few, thin dipole-like projections being the rule (Figure 43). An indication of the distribution of the glide regions as projected on the prism plane is given by Figure 44, which is taken at four times lower magnification than Figure 43. Dislocations on the basal plane form the already familiar bundles of edge dislocations, dipole formations similar to Figure 39, loops, etc. Figures 45, 46, and 47 give an indication of the variety and complexity of formations. Series of large dislocation links of high regularity were observed with radii of 0.5 to 2μ. The dislocation structures in Figure 45 deserve particular attention. The straight sections of the kinked dipoles lie

44

Figure 40 - Dislocation array as projected on a (10$\bar{1}$0) plane. 40,000:1.

Figure 41 - Cracks on the surface of a high purity tensile crystal before straining. 260:1.
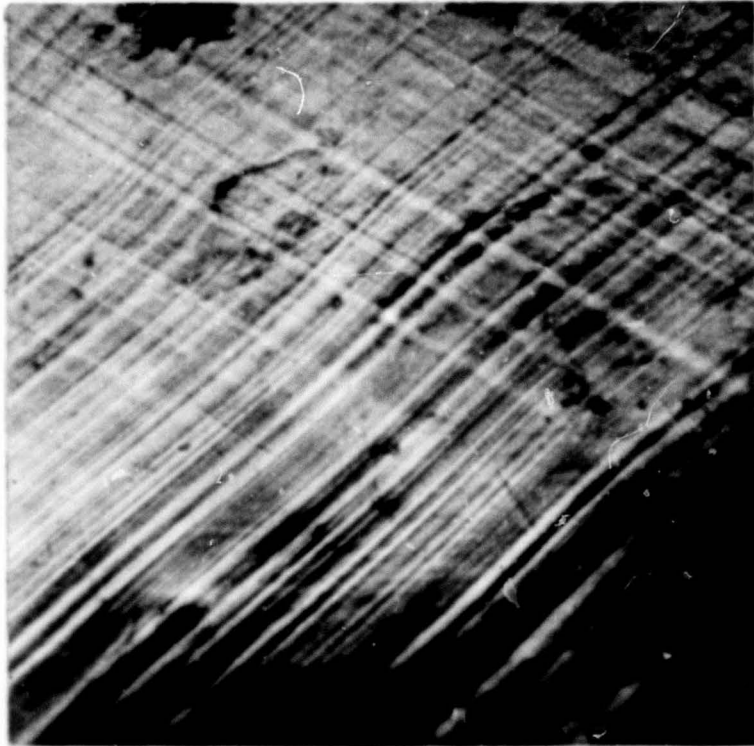
Figure 42 - Double slip at the surface of a tensile specimen after straining. 420:1.
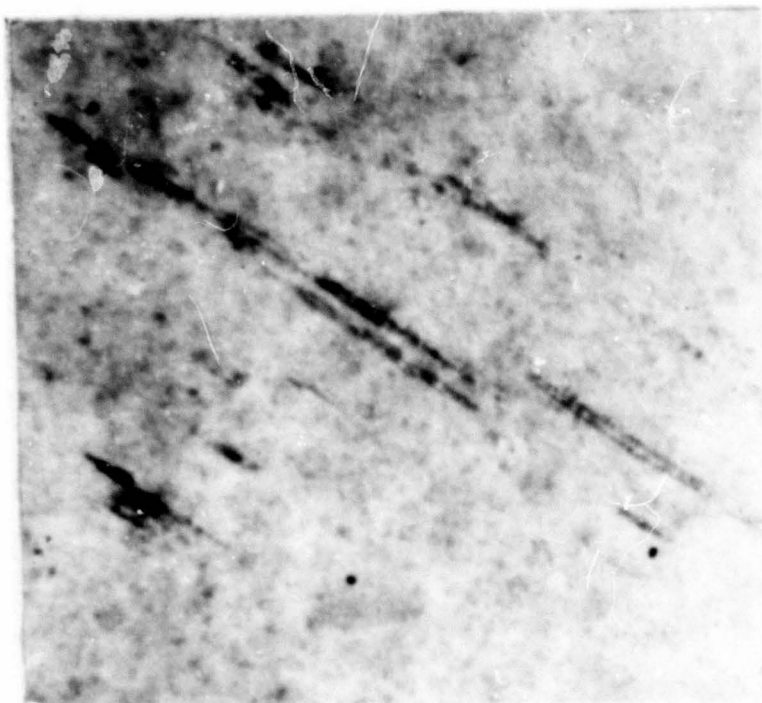
Figure 43 - Dislocation pattern projected on a (10$\bar{1}$0) plane. Note the formation of dipoles. 40,000:1.

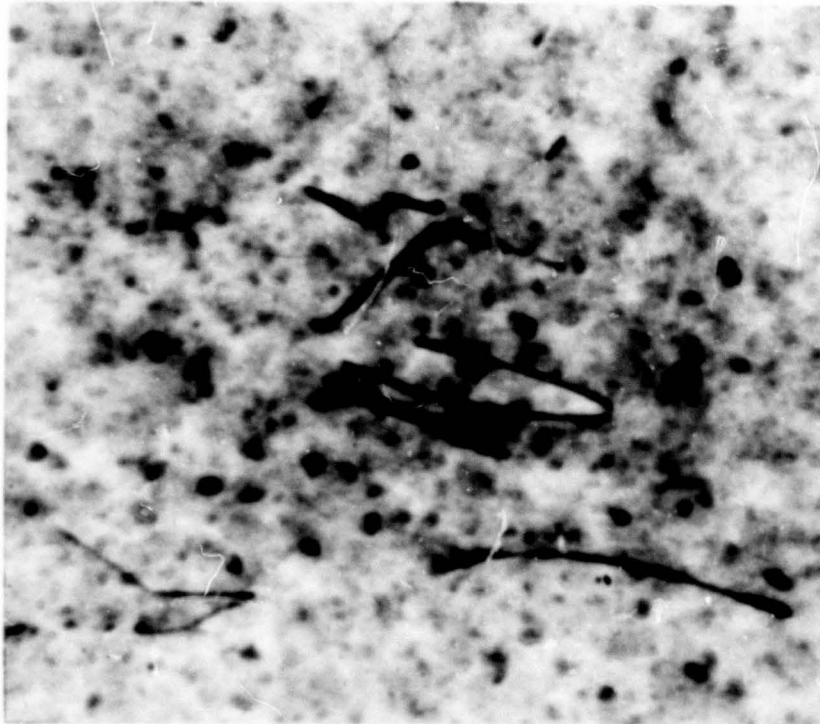Figure 44 - Dislocations as seen on a (10$\bar{1}$0) plane at lower magnification. 10,000:1.

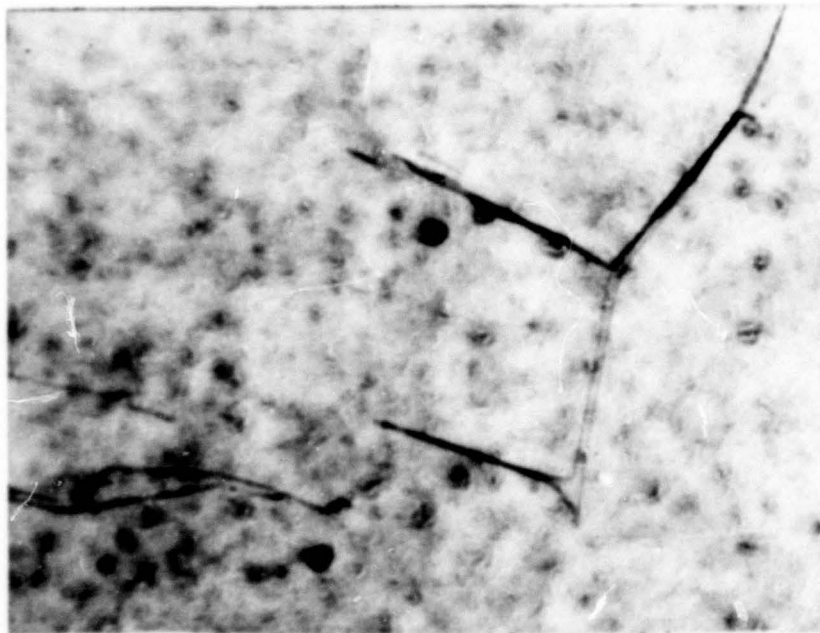Figure 45 - Kinked dipoles, viewed in the direction of the c-axis. 40,000:1.

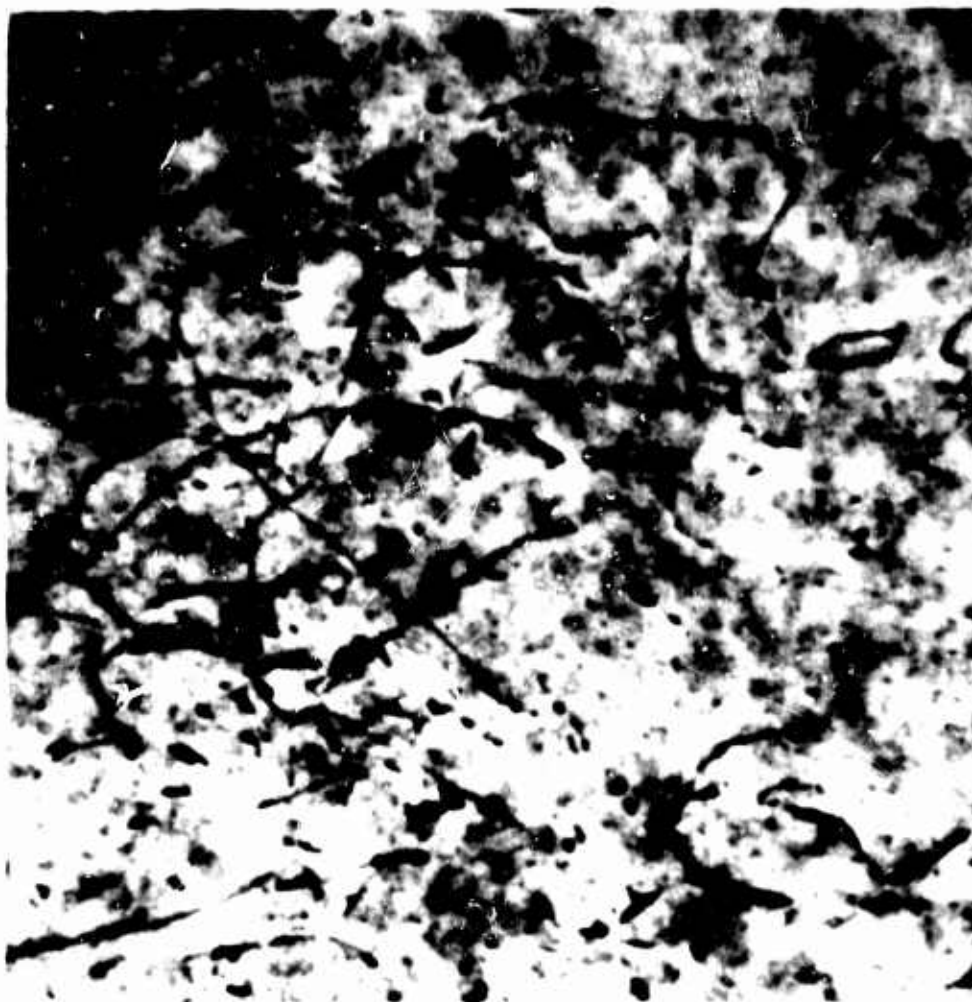Figure 46 - Dipole formation in high purity specimen. 40,000:1.

Figure 47 - Irregular dislocation array with loops and dislocation
arcs in a high purity crystal. 40,000:1.

in <10$\bar{1}$0> directions in such a manner that one of these directions is perpendicular to one of the two active glide vectors (i.e., parallel to the majority of "bundles" and long dipoles); the other direction is determined by the resultant of the two active glide vectors. Kinked dipoles of this type are quite common in beryllium crystals and have also been found in polycrystalline Pechiney flake. Not always do double dislocations lie in an orientation with low crystallographic indices. In Figure 46, only the dislocation branches approximately in the lower center of the micrograph and in the section in the left hand corner are perpendicular to a possible glide direction, while the resolved dipole in this micrograph points to [12$\bar{3}$0]. That the components of this dipole are parallel and straight over a length of almost 1μ indicates an effective locking mechanism. Dipoles of this type sometimes have been seen to be "twisted." Occasional dislocation movement was detected during the electron microscopic study. Dislocations moved rapidly, but only over short distances, and appeared to be locked again in their new position.

IX. DISCUSSION AND CONCLUSIONS

This investigation was initiated in order to examine the relationship between dislocations and the failure of beryllium crystals. The discussion will endeavor to evaluate the experimental material within the given scope, and no attempt will be made to cover completely the numerous observations which have a bearing on the theory of dislocations.

With regard to the brittleness problem of beryllium, the following conclusions had been drawn from observations on dislocations after some preliminary experimental work (Ref. 9): (1) Dislocation pinning, and, to some extent, dislocation tangling, are the predominant features in the dislocation behavior of beryllium crystals produced from Pechiney flakes or from commercial material; (2) The frictional force acting on moving dislocations in Pechiney flake and commercial material is high as compared to hexagonal metals with a c/a ratio larger than the ideal close packing; (3) The stacking fault energy is high, i.e., about 50 ergs/cm^2 or more.

The comprehensive work carried out in the course of this investigation on specimens prepared from commercial material, Pechiney flake, and high-purity material has confirmed the above statements. Extensive evidence for the pinning and tangling of dislocations has been obtained, and examples of patterns are presented by electron micrographs in Sections VI and VII, which describe the results on Pechiney flake and commercial beryllium. Also, the fact that dislocations strongly prefer to lie parallel to crystallographic directions in samples, regardless of purity, strengthens our contention that the frictional force on moving dislocations is high. The third point - the question of stacking fault energy - shall be elaborated on in more detail.

A direct measurement of the stacking fault energy can be obtained through measurements on "open" nodes in dislocation networks. V. D. Scott (Ref. 10) claims to have seen open nodes in beryllium and concluded that the stacking

fault energy is rather small. The stacking fault energy $\gamma = Gb^2/2R$, with G the modulus of rigidity, b the Burgers vector, and R the radius of the stacking fault forming the open node (see Figure 48). In order to obtain a decisive answer to this question, deformed specimens (commercial purity beryllium) were polygonized for 30 minutes at 800°C and examined by diffraction electron microscopy. Numerous networks were observed, but no evidence for open nodes was obtained. However, occasionally hexagonal networks exhibited contrast at one side of the threefold nodes as indicated in Figure 48 (shaded area). Obviously, this contrast is not due to "open" nodes, but is caused by a diffraction effect because of the distortion of the lattice near the nodes, provided that the orientation of the specimen is asymmetrical with regard to the relation between network and diffraction condition. It is known that impurities can change the stacking fault energy to a considerable extent. Therefore, it is advisable not to generalize when referring to stacking fault energies in beryllium, since little is known about the local distribution of impurity atoms in this metal.

The brittle fracture of commercial and Pechiney flake beryllium is generally a cleavage failure along the basal plane. All microscopical theories of brittle fracture assume the nucleation of a crack through (1) internal stress concentrations or (2) through the formation of voids. Stress concentrations caused by dislocation mechanisms all employ dislocation groups on one or, less frequently, on two intersecting glide planes, as well as small angle boundaries ending within the crystal, and, finally, interactions of dislocations with boundaries. The dislocation patterns observed by diffraction electron microscopy will now be assessed in the light of these concepts.

The present study had been designed to compare the dislocation patterns in brittle beryllium with those of ductile beryllium, assuming that substantial differences would exist. In this respect, the investigation may be considered successful since, indeed, marked differences in dislocation behavior between high purity beryllium, on the one hand, and commercial and Pechiney flake material, on the other, have been found.

The most prominent feature in the arrangement of glide dislocations in high purity beryllium is their grouping into flat "bundles" parallel to $\langle 1\bar{1}00 \rangle$, i.e., they consist of edge dislocations. A considerable proportion are dipoles, which is in good agreement with the fact that no internal stresses originating from the clusters could be detected by diffraction contrast techniques. In addition, many dislocations are present having fairly large link lengths and often being almost straight. In contrast to this dislocation pattern, the distribution of glide dislocations in Pechiney flake and commercial beryllium is quite different regarding both the appearance of individual dislocations as well as their clustering. The arrangements frequently observed are irregular boundaries, possibly similar to those observed in pure fcc metals, and large parts of the crystal volume filled with glide dislocations at random. In addition, a smaller number of dislocation groups and small angle boundaries were seen, and these observations, in particular, are pertinent to the brittleness problem. Evidence provided by diffraction contrast indicates not only that slight differences in orientation exist between crystal volumes separated by the irregular boundaries, but also that the dislocation clusters produce internal stresses. It must be concluded then that dislocations of one sign are primarily present in these groups.
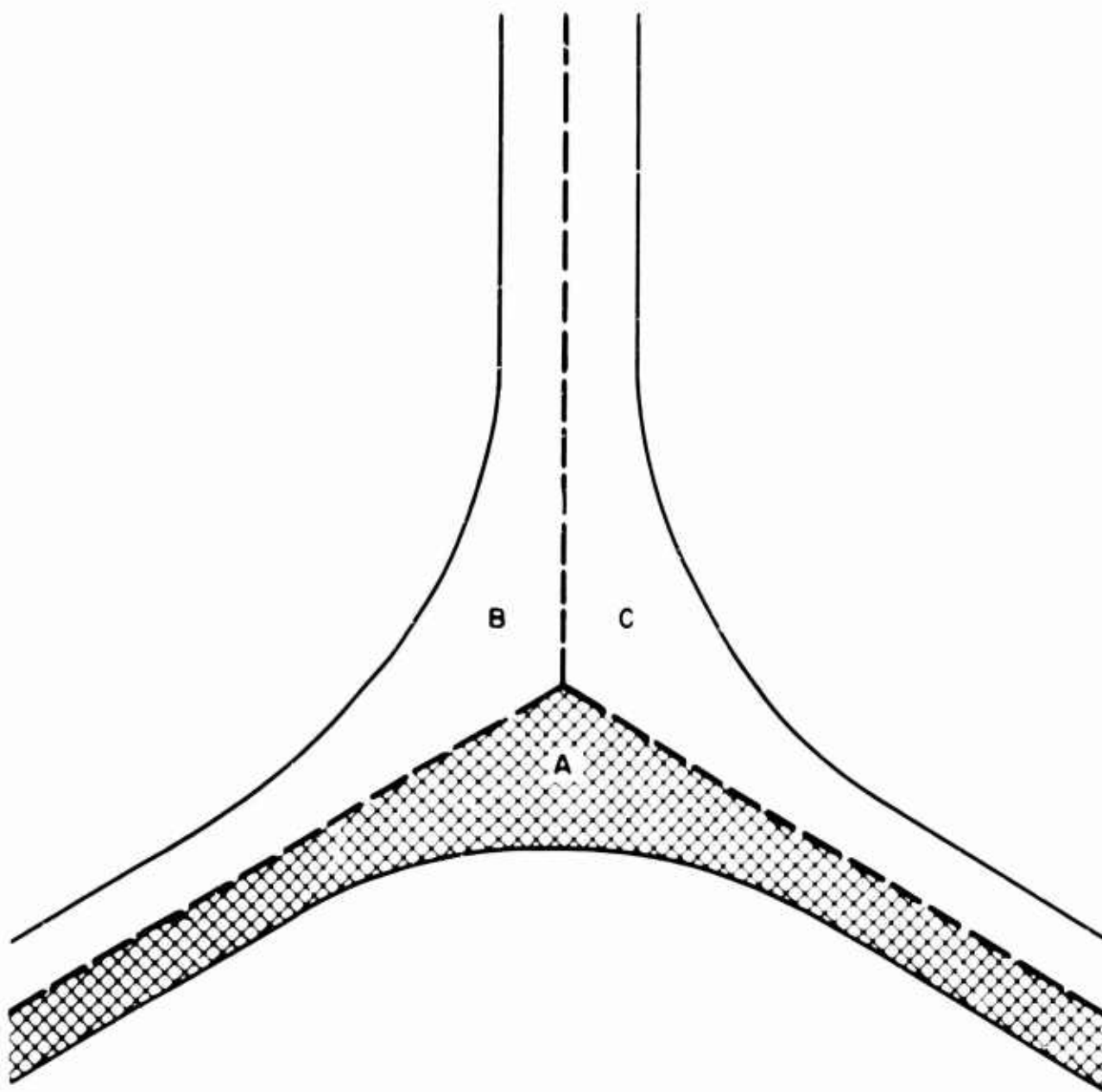
Figure 48 - Schematic drawing of open node in a dislocation network. Only shaded area A has been observed in this investigation to show diffraction contrast, while for dislocations with small stacking fault energy areas B and C also should have contrast, comparable to A.

The cause of the different dislocation behavior in brittle as compared to ductile beryllium is undoubtedly due to the pinning of dislocations. A preponderance of pinning points along the dislocation line not only will be responsible for an increase of stress to move the dislocations as a whole, but also they provide for many potential dislocation sources. The first effect causes the flow stress of brittle beryllium to be one order of magnitude higher than for the ductile material; thereby, the sum of applied and internal stress a priori is very high, and already at the beginning of plastic deformation the combined stress is in the range of the fracture stress. The operation of dislocation sources at these high stresses will undoubtedly be by the Frank-Read mechanism, which would easily explain the presence of dislocation groups consisting of dislocations of one sign in the brittle material. The high impurity content of brittle beryllium suggests that the pinning of dislocations is caused by impurities which are in solution. Another reason for the production of dislocation groups was indicated by the observation of larger precipitates which, because of their different coefficient of thermal expansion, originate many dislocation loops.

It has become increasingly clear in the course of this study that impurities and vacancies have a profound influence on the multiplication of dislocations in beryllium containing different amounts of impurities. Since the failure of beryllium commonly is by cleavage, the influence of dislocation boundaries and particular dislocation groups and the interaction of the latter with the former is of greatest importance for the separation of two close-packed planes, i.e., the formation of crack nuclei. The results obtained so far support the contention that the detailed mechanism of crack formation in beryllium of different impurity content can be resolved by applying the diffraction electron microscopy method.

REFERENCES

1) H. G. F. Wilsdorf and D. Kuhlmann-Wilsdorf, Phys. Rev. Letters, $\underline{3}$, 170, (1959).

D. Kuhlmann-Wilsdorf, R. Maddin and H. G. F. Wilsdorf, "Strengthening Mechanisms in Solids", ASM, 1962, p. 137.

D. Kuhlmann-Wilsdorf and H. G. F. Wilsdorf, Proc. of the Conf. on "Electron Microscopy and Strength of Crystals," Berkeley, 1961. John Wiley, 1963, p. 575.

2) J. T. Fourie and H. G. F. Wilsdorf, J. Appl. Phys., $\underline{31}$, 2219 (1960).

3) D. Kuhlmann-Wilsdorf, Phys. Rev., $\underline{120}$, 773 (1960).

4) A. R. Kaufmann, "The Metal Beryllium", ASM, Cleveland, 1955, p. 367.

5) A. Saulnier, J. Nucl. Mat. $\underline{2}$, 299 (1960).

6) V. Damiano and M. Herman, Trans. AIME, $\underline{215}$, 136 (1959).

7) Y. T. Chou, J. Appl. Phys. $\underline{33}$, 2747 (1962).

8) W. Pfeiffer, Phys. Stat. Sol., $\underline{2}$, 1727 (1962).

9) H. G. F. Wilsdorf and F. Wilhelm, Paper 41, Conference on Metallurgy of Beryllium, Inst. of Metals, London (1961).

10) V. D. Scott, Discussion, Conference on Metallurgy of Beryllium, Inst. of Metals, London (1961).